ECN

Energy research Centre of the Netherlands

Individual Pitch Control for Large scale wind turbines

Multivariable control approach

Kausihan Selvam

ECN-E–07-053

Abstract

In the next decennia, upscaling even towards 10 MW wind turbines may be necessary to lower the costs of offshore wind energy. This requires considerable reductions of turbine loads. Variable speed turbines with active pitch control are most favorable and prevailing nowadays. Currently, the turbine blades are turned collectively to limit the excess of wind power and to regulate the rotor speed above rated wind conditions. To reduce the blade and tower loads, it has been shown that Individual Pitch Control (IPC) is much promising. A multivariable control concept using advanced feedback-feedforward control method is implemented for IPC and is compared with the traditional scalar control concept. The advantage of using such a control concept is also shown.

Keywords

Individual Pitch Control, Multivariable control, Feedback-Feedforward control

Acknowledgement

This master thesis has been carried out as part of the requirement for obtaining the degree of Master of Science in Systems and Control Engineering. This report describes the results of my graduation project “Individual Pitch Control for large scale wind turbines: Multivariable control approach”carried out at Energy research Centre of the Netherlands (ECN) governed by the Delft Center of Systems and Control (DCSC).

A large number of individuals have assisted me in preparing this work. In particular I would like to thank prof. M. Verhaegen and ir. T.G. van Engelen for coming up with the first ideas of this assignment. I would also like to acknowledge them and other members of DCSC and ECN for giving me an opportunity to work on such an interesting project. I would like to thank ir. T.G. van Engelen for providing the models and pictures that have been used extensively in this thesis and also for the matlab program files that were used in the course of this thesis. I would like to thank Dr. S. Kanev for his insights and help with random walk model and H_2 control. I would also like to thank him for the coaching he provided and time he spent in discussions and the help he provided without which this thesis would not have been possible. I would also like to thank ir. E.L. van der Hooft (ECN), Dr. Stoyan Kanev (ECN) and ir. D.A.J. Wouters (ECN) in guiding me and providing a helping hand while working on the project and the report and also for co-reading the reports. I would also like to acknowledge the contributions made by ir. J.W. van Wingerden (DCSC) at various stages of the thesis and preparation of the report. I would also like to acknowledge the help provided by ir. C. Lindenburg in teaching me basics of fatigue analysis. Finally I would also like to acknowledge the support provided by others who have all inspired this work.

Kausihan Selvam

summary

The appetite for energy in Europe and the World in general, is increasing at a tremendous rate. Wind energy, a renewable form of energy, needs to be utilised to fill this appetite for energy. But the disadvantage of wind energy is that it is expensive when compared to the direct costs fossil fuels. Hence to reduce the cost of production the general idea is to build larger wind turbines and to move them to offshore locations where the wind speed is higher. But for a successful implementation of such schemes certain issues such as maintenance and reliability issues of wind turbines should be solved. The thesis "Individual Pitch Control for large scale wind turbines"aims at providing a solution for one of the above issues - reduction of fatigue loads on the rotor blades and thus maintenance costs. In order to achieve the desired results the following issues were tackled.

The previous researches that have taken place in the field of Individual Pitch Control for both the helicopter industry and the wind industry were reviewed. Then a suitable control approach was chosen based on prior reviews and results. This control approach that will be discussed in this thesis is multivariable H_2 control with feedforward wind disturbance rejection.In a feasibility study the above chosen control technique is analysed, based on a simple wind turbine model, and is compared with scalar control technique adopted by [van Engelen and Van der Hooft (2003)]. A more detailed analysis of these two control techniques is performed using TURBU, where a detailed specification of a 2.5 MW wind turbine. Finally the conclusion of the controller design and some recommendations for controller performance improvement are provided.

The most important conclusion is that we can use advanced feedback-feedforward multivariable control designs for reducing the 1P and 2P blade loads.

This report has been presented as a master of Science Thesis at TU Delft on July 25, 2007.

List of symbols

$HAWT$	Horizontal Axis Wind Turbines
IPC	Individual Pitch Control
HHC	Higher Harmonic control
CPC	Collective Pitch Control
ECN	Energy research Centre of Netherlands
$SISO$	Single Input Single Output systems
$MIMO$	Multiple Input Multiple Output systems
PI	Proportional and Integral
LQG	Linear Quadratic Gaussian
R_b	Rotor Blade radius
v_{fl_i}	Blade effective wind speed
$\theta_1, \theta_2, \theta_3$	Pitch angles for blades 1, 2 and 3
θ_{cm}	Pitch angles in coleman domain for rotor orientation (caxial, tilat and yaw)
ψ_1, ψ_2, ψ_3	Azimuth angles of blades 1, 2 and 3
x_{fa}	fore-aft displacement of the tower
x_{sd}	Sidewards displacement
$\delta M_{x,i}$	Leadwise blade root bending moments of the blades (i = 1,2,3)
δM_t	Tilt moment at rotor centre
$\delta M_{z_i^{cm}}$	Blade bending moments in the coleman domain (i = 1,2,3)
u_{cm}	Wind in Coleman domain
Ω	Rotor speed
J	Inertia of the rotor
δT_g	Generator torque
δT_a	Aerodynamic torque
1P 2P 3P	once per/twice per/thrice per revolution
δF_a	Axial force
δF_s	Sidewards force
m_{tw}	Mass of the tower
s_{tw}	spring coefficient of the tower
d_{tw}	damping coefficient of the tower

Contents

1 Introduction

1.1 Background

The world of today is energy hungry and the appetite for energy will only increase in the future as and emerging countries such as Brazil, India and China, will increase pressure on the already high energy demand from developed countries. The dramatic increase in fuel prices and the economic and geopolitical risks associated with imported fuels have moved to the top of the political agenda. Meanwhile, the negative effects of climate change and pollution are becoming ever more apparent. The rise of world temperature is no longer a question of "if"but a question of "how much"and "by when", as clearly pointed out by the Intergovernmental Panel on Climate Change, [Watson (2001)] widely taken as the 'consensus of the scientists'. Climate change is also disturbing the water cycle, which has dramatic consequences for electricity production patterns. The global energy challenge of our time is to tackle the threat of climate change, meet the rising demand for energy and to safeguard security of energy supplies. Wind energy is one of the most effective power technologies that is ready today for global deployment on a scale that can help tackle these problems.Wind power can be installed far quicker than conventional power stations. This is a significant factor in economies with rapid growth in electricity demand.
The current trend in wind energy is to place the wind turbine in offshore locations. This has many advantages such as availability of higher wind speeds and less turbulence at offshore locations, size of rotors can be increased without the need to worry about lack of space and affecting agricultural and living spaces. Moreover a new estimate from researchers at Stanford University puts the figure of energy production capacity available worldwide in offshore locations to 72 TW [Archer and Jacobson (2005)].

1.2 Motivation

Presently the wind turbine manufacturers are involved in producing wind turbines with higher rated powers which means rotors with larger diameter. The sizes of the rotor diameter of a commercial wind turbine with rated power capacity of 3 MW is about 100 to 110 meters. Prototype wind turbines (5 MW) with a rotor diameter up to 126 meter exist. But increasing the rotor diameters also introduces asymetric loading of the rotor blades [Hansen (2000); van Kuik et al. (2003)]. This combined with the fact that maintenance and constant supervision of wind turbines at offshore locations is expensive and very difficult, means that we need a more reliable control technique for fatigue and load reduction. Many control techniques have been put forward for this purpose which include individual pitch control [Bossanyi (2003a); Caselitz et al. (1997); van Engelen and Van der Hooft (2003); Larsen et al. (2005)].
Individual pitch control is an attractive option for load reduction for many reasons [Bossanyi (2003a)], some of which are

- Commercial turbines nowadays have individual pitch actuators for each rotor blade, hence no physical adjustment needs to be made for implementation of IPC.
- Load reduction through modern control systems is more attractive and cheaper in comparison with designing mechanical systems to cope with large loads.
- The technique aims to reduce the asymmetric loads due to wind speed variations across the rotor disc, and these loads are becoming more significant as turbine rotors get larger with respect to the size of typical turbulent eddies in the wind.

1.3 Problem formulation

At ECN, research on individual pitch control has already been done using classical control techniques [van Engelen and Van der Hooft (2003)]. Their approach [van Engelen and Van der Hooft (2003)] is based on the decoupling of the multivariable control problem into three time invariant scalar controllable loops by a coordinate transformation under the assumption that these three scalar loops are completely independent of each other.

- the collective control loop (rotor speed control)
- the tilt control loop
- the yaw control loop

The feasibility study was based on a simplified design and evaluation model as generated by TURBU, ECN's linear analysis and simulation code for Horizontal Axis Wind Turbines (HAWT) [van Engelen (2007)]. Higher blade bending and higher tower bending modes were taken out of consideration, even as phenomena like unsteady aerodynamics. Quick scans show that the three control loops are not fully independent (orthogonal) in simulations with more detailed models.

The aim of this thesis is to investigate a multivariable control technique that could be used for IPC that takes into account the non orthogonality of the scalar loops.

This problem has solved in four steps as follows.

- analysis of various IPC methods.
- analysis of various candidate control techniques.
- feasibility study of a chosen multivariable control technique on a simple wind turbine model.
- stability analysis and performance improvement with the modern control technique compared to the original three scalar control loop.

1.4 Outline

This chapter provided an introduction into the subject of this thesis and presented the problem formulation. The remainder of this report consists of five chapters. A brief overview of these chapters will now be presented.

- Chapter 2 describes the development of IPC from the helicopter industry and how IPC is utilised in the field of wind energy. A brief overview of the multiblade coordinate transformation that has been utilised in various research papers is also provided in this Chapter.
- Chapter 3 discusses the necessary theoretical background of multivariable control techniques including decoupling of the multivariable problem into scalar problems whose results will also be provided in Chapter 5.
- Chapter 4 describes the method of control design for multivariable control. In this chapter a feasibility study, showing how a wind turbine model for multivariable control is generated, is discussed. Furthermore comparison between the multivariable control and the classical control approach is made to study the advantages of the new approach.
- In Chapter 5, the final analysis in TURBU, of the new control approach is compared with classical control approach to show the importance of taking into account the non-orthogonality of the system.
- Finally, the main conclusions from this research will be drawn and recommendations for future work are given in 6.

2 Introduction to Individual Pitch Control (IPC)

2.1 Introduction

Blade pitch control has primarily been used to limit aerodynamic power in above rated wind speeds in order to keep the turbine within its design limits and to optimize energy capture at below rated conditions. Collective pitch control techniques have been successfully utilised for this purpose [Bossanyi (2000); Van der Hooft et al. (2003); Wright and Balas (2002)]. But as rotor size increases there is an increased interest in utilising pitch control to alleviate loads experienced by wind turbines by pitching the blades individually. The basic technique of individual pitch control is borrowed from the helicopter industry where scientists like Johnson [Johnson (1982)] and Lovera [Lovera et al. (2003)] have done work in this field.

2.2 Individual pitch control in the helicopter industry

Load reduction using blade pitch action has been investigated upon for a long time in the rotor craft industry. Johnson has worked on the problem of advanced aerodynamics and multi cyclic pitch control (precursor to the modern cyclic pitch control problem) [Johnson (1982)]. Lovera in [Lovera et al. (2003, 2004)] analyse the stability of IPC and Higher Harmonic Control (HHC) for rotor helicopters based on discretized periodic models derived through finite elements, with modal coordinate transformation using T-matrix algorithm [Lovera et al. (2003)] which converts the 1p and its harmonic responses in a fixed frame of reference . In [Lovera et al. (2003)] the authors discuss the performance of a SISO periodic HHC compensator. This discussion is followed by a generalised approach to implement multi-harmonic signals to attenuate several components of the vibratory load in MIMO HHC. In [Lovera et al. (2004)] the same analysis is extended with the inclusion of discrete elements in the HHC loop. In this paper Lovera conclude that non inclusion of the discrete elements is unconservative in nature caused due to sampling delay. The other important aspect of Lovera's work is the derivation of Harmonic Transfer Function (HTF) which can be utilised in derivation of both SISO and MIMO models.

2.3 Cyclic pitch control

This is the most simplistic method for attenuating loads, especially those caused at 1P frequencies. The basic principle of cyclic pitch control is given by Larsen in [Larsen et al. (2005)] as "Measure mean tilt rotor and yaw moments and compensate by an aerodynamic moment created by a cyclic pitch variations that are 120° out of phase (3 bladed machine)". In this method the rotating blade flap and edgewise blade root moments are converted into non rotating rotor coordinates as given in Eq. 2 and Eq. 3

$$M^R_{x,i} = M^B_{x,i}\ \cos(\theta_i) + M^B_{y,i}\ \sin(\theta_i) \tag{1}$$

$$M_{tilt} = \sum_{i=1}^{B} M^R_{x,i}\ \cos(\phi_i) \tag{2}$$

$$M_{yaw} = \sum_{i=1}^{B} M^R_{x,i}\ \sin(\phi_i) \tag{3}$$

where $M^B_{x,i}$ and $M^B_{y,i}$ are the flap and edgewise blade root bending moments of blade i, with ψ_i being the azimuth angle of the respective blade i and θ_i is the pitch angle of the blade. M_{tilt} and M_{yaw} represent the tilt and yaw moments at the rotor centre. Then these moments are compensated and the resulting pitch action is a combination of θ_{yaw} and θ_{tilt} given by Eq. 4.

$$\theta_{cyc,i} = \theta_{tilt}\ \sin(\phi_i + \Phi) + \theta_{yaw}\ \cos(\phi_i + \Phi) \tag{4}$$

Here θ_{yaw} and θ_{tilt} are the compensating pitch action for yaw and tilt moment respectively. the small phase shift Φ is introduced to compensate for the actuation delay.
Wright in [Wright (2004)] implements a state space method, with the azimuth angle ψ as one of the states, for disturbance rejection which boils down to cyclic pitch control as the approach is limited to 1P effects. Similar approach is followed by Stol [Stol (2003)] and Balas [Wright and Balas (2003)]. Their approach is based on developing a composite state-space controller for a periodic model by inclusion of states containing the change in blade flap angles β_i) and the rotor azimuth angle (ψ) and their derivatives as given by

$$\begin{aligned} \dot{x}(\psi) &= Ax(\psi) + Bu(\psi) + B_d u_d && (5) \\ y &= Cx(\psi) && (6) \end{aligned}$$

where

$$\begin{aligned} x &= \left[\Delta\psi \;\; \Delta\beta_1 \;\; \Delta\beta_2 \;\; \Delta\dot{\psi} \;\; \Delta\dot{\beta}_1 \;\; \Delta\dot{\beta}_2\right] && (7) \\ u &= \left[\Delta T_g \;\; \Delta\theta^T\right]^T && (8) \\ u_d &= \Delta w && (9) \end{aligned}$$

and the state matrices (A, B, B_d) are periodic in nature.

2.4 Individual pitch control for load reduction

Cyclic pitch control can be used to reduce deterministic loads caused by aerodynamic wind shear loading, tower shadow and yaw misalignment. But they cannot alleviate stochastic disturbances caused by turbulence. In recent years research has been done in this area by Bossanyi [Bossanyi (2003b,b)] and Larsen [Larsen et al. (2005)]. Bossanyi's method is based on measurement of blade root loads and transforming them into a mean value and variations on two orthogonal axis using "d-q axis transformation". The two orthogonal axes are known as direct and quadrature axes and the transformation matrix that transforms the rotating blades to quadrature axes is given by Eq. 10

$$\begin{pmatrix} \beta_d \\ \beta_q \end{pmatrix} = \begin{pmatrix} \frac{2}{3} & 0 \\ 0 & \frac{2}{3} \end{pmatrix} \begin{pmatrix} \cos(\theta) & \cos(\theta + 2\pi/3) & \cos(\theta + 4\pi/3) \\ \sin(\theta) & \sin(\theta + 2\pi/3) & \sin(\theta + 4/3) \end{pmatrix} \begin{pmatrix} \beta_1 \\ \beta_2 \\ \beta_3 \end{pmatrix} \qquad (10)$$

It is assumed that there is no interaction between the two axes. Hence classical SISO techniques could be used to control the system.
One of the disadvantages involved in this method is the possible time-delay caused while measuring the blade loads (the blade acts as a filter - as concerns to the realisation of pitch angles). Thus a phase mismatch in this system could increase the load rather than decrease it. To overcome this problem Bossanyi introduces a phase shift in the modulated feedback signals of β_d and β_q, such that the 'around -1p'variation in the three pitch angles is obtained by modulation of the fed back β_d and β_q with azimuth angle is $\theta + \Delta\theta$, where $\Delta\theta$ compensates for actuator delay. Larsen *et al* [Larsen et al. (2005)] recipe to overcome this problem is to measure inflow parameters "angle of attack"and "relative velocity"and design an individual pitch compensator based on these measurements rather than blade load measurements. Their reasoning is based on the theory that strong correlation exists between angle of attack and blade bending moment (flap).
In the local blade flow method two control actions based on separation of angle of attack measurements and relative velocity measurements are implemented. The authors have implemented a PI based feedback control of pitch angle based on the error between the angle of attack of a single blade and average angle of attack. For relative velocity based control action, a model-based feed forward gain is calculated and implemented as given in equation Eq. 12

$$\begin{aligned} V_x &= V_{rel} cos(\alpha + \theta) && (11) \\ \theta_{\delta_i,b} &= (V_x - V_{x,avg}) K(\omega, \theta_{coll}) && (12) \end{aligned}$$

where V_x is the wind speed in-plane with the rotor which is a function of relative velocity or rotor centric velocity V_rel, blade pitch angle θ and angle of attack α, $V_x - V_{x,avg}$ is the error between the in-plane relative velocity on the single blade and the average in-plane relative velocity of the three blades and $K(\omega, \theta_{coll})$ is the feedforward gain function. The gain function is based on calculations of skew inflow with the turbine equipped with a cyclic pitch regulator.
This method, though has some disadvantages. First, the measurement of velocity using pitot tube has reliability and robustness issues. Second, the effect of nodding and naying of the turbine might also cause discrepancies in the measurement of relative velocity and thereby the correction may actually increase the load rather than decrease it.

2.5 Higher harmonic control

Cyclic pitch control and individual pitch control techniques explained in Sec. 2.3 and Sec. 2.4 have been developed to reduce 1P loading. It is also possible to reduce 2P and 3P loading. This is known as higher harmonic control. There has been some research done in this field in the helicopter industry by Marco Lovera [Lovera et al. (2003)]. In the field of wind energy research has been done by Bossanyi [Bossanyi (2005)] and van Engelen [van Engelen and Van der Hooft (2003)].
Bossanyi's work involves the implementation of a feedforward notch filter to remove the 3P component from the input fixed frame load or in other words the amplitude and phase of the 3P response of the compensator is adjusted to 2P and 4P effects of the fixed frame loads which could then be eliminated using 'd-q axis'approach as in [Bossanyi (2003b)].
The other approach for HHC(higher harmonic control) is to provide different feedback loops for 2P and 3P effects. This approach is followed by van Engelen in [van Engelen and Van der Hooft (2003)]. The *multi-blade coordinate transformation* as explained by Coleman [Coleman and Feingold (1958)] is utilised in this approach to map the blade variables into 'fixed coordinate system'(superscript^{cm}) as given in Eq. 13

$$\begin{bmatrix}\theta_1\\ \theta_2\\ \theta_3\end{bmatrix} = \begin{pmatrix} 1 & \sin\psi_1 & \cos\psi_1\\ 1 & \sin\psi_2 & \cos\psi_2\\ 1 & \sin\psi_3 & \cos\psi_3 \end{pmatrix} \cdot \begin{bmatrix}\theta_1^{cm}\\ \theta_2^{cm}\\ \theta_3^{cm}\end{bmatrix} \tag{13}$$

$$\begin{bmatrix}M_{z_1}^{cm}\\ M_{z_2}^{cm}\\ M_{z_3}^{cm}\end{bmatrix} = \begin{pmatrix} \frac{1}{3} & \frac{1}{3} & \frac{1}{3}\\ \frac{2}{3}\sin\psi_1 & \frac{2}{3}\sin\psi_2 & \frac{2}{3}\sin\psi_3\\ \frac{2}{3}\cos\psi_1 & \frac{2}{3}\cos\psi_2 & \frac{2}{3}\cos\psi_3 \end{pmatrix} \cdot \begin{bmatrix}M_{z_1}\\ M_{z_2}\\ M_{z_3}\end{bmatrix} \tag{14}$$

where $M_{z,i}$ and ψ_i are the blade flap moments and the azimuth angles of blade *i* respectively.
It is assumed that uncoupled transfer functions can be derived for the rotor speed Ω and tilt- and yaw wise multiblade coordinates ${M_{z_1}}^{cm}$ and ${M_{z_2}}^{cm}$ of the flapwise moments from this design model. Hence a LTI scalar control design could be implemented for each multi blade coordinate angle ${\theta_i}^{cm}$. A similar approach has been implemented to reduce 2P and 3P loads.

3 Candidate multivariable control techniques

In this chapter multivariable controller techniques that are available in literature that pertain to wind turbine control design are discussed. In classical control techniques the control designs are focused on single input and single output. Other signals in the control loop are considered to be disturbance signals. But in reality these disturbances tend to have signals from other loops that interact with the designated control loop. Such systems are generally known as MIMO(multi-input multi-output) systems. In practice all systems are MIMO in nature.
Frequently you encounter systems where inputs and outputs can be grouped into pairs and treated as separate SISO (single input single output) sub systems that tend to form the MIMO system. All the research on wind turbine control refered to in Chap. 2 utilises this fact to design simple SISO controllers. But, ever so often non negligible interactions between the multiple inputs and outputs can occur. In these cases a control design method which takes into account such interactions, needs to be applied.

3.1 Introduction to multivariable systems

A multivariable or a MIMO system is a system that contains more than one input or output. Consider a system with *m* inputs an *l* outputs.Then the basic transfer function model becomes $y(s) = G(s)u(s)$ where y is a $l \times 1$ vector, u is a $m \times 1$ vector, and $G(s)$ is a $l \times m$ matrix transfer function.
A MIMO system can be described using state space ideas similar to that of a SISO system. The difference being the inclusion of vector inputs and outputs instead of scalar values. If the system has input vector $u(t) \in \mathbb{R}^m$ and an output vector $y(t) \in \mathbb{R}^l$, then its state space model is written as

$$\begin{aligned} \dot{x}(t) &= \mathbf{A}x(t) + \mathbf{B}u(t) \\ y(t) &= \mathbf{C}x(t) + \mathbf{D}u(t) \end{aligned} \tag{15}$$

In Laplace domain the system is defined as a transfer function matrix instead of a single transfer function. The transfer function matrix of the system **G**(s) is defined as follows

$$\mathbf{G}(s) \triangleq \mathbf{C}(s\mathbf{I} - \mathbf{A})^{-1}\mathbf{B} + \mathbf{D} \tag{16}$$

For more details on the representation of MIMO systems, the reader is refered to [Skogestad and Postelwithe (2005)]. The general description of the system in this report is the standard transfer function matrix model as described in Eq. 16 unless mentioned.

3.2 Control of multivariable system

3.2.1 Decentralized control design

The simplest approach to a multivariable control design is the use of a block-diagonal controller $K(s)$ as shown in Fig. 1. This is a straight forward process if the system $G(s)$ is also block diagonal, because then the whole system is in turn a collection of independent SISO subsystems. But if the the system is non diagonal then a precompensator $W(s)$ designed so as to counteract the interactions is added to the system so that the new system $G_s(s)$ is diagonal in nature as shown in Eq. 17 and Fig. 2.

$$G(s) = G_s(s) \cdot W^{-1}(s) \tag{17}$$

Hence the controller becomes

$$K_s(s) = W(s) \cdot K(s) \tag{18}$$

This type of decoupling control occurs when compensator W is chosen such that $G_s = GW$. When the system is decoupled for all frequencies it is known as dynamic decoupling. For example $W(s) = G^{-1}(s) \cdot G_{diag}(s)$ [Skogestad and Postelwithe (2005)]. When the overall system is made

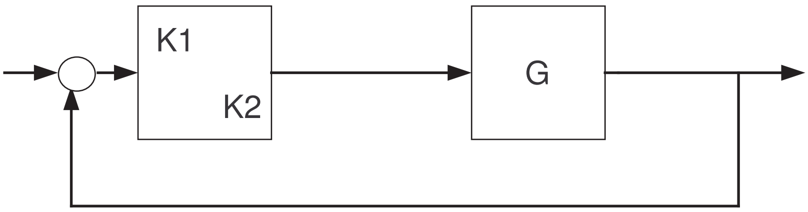

Figure 1: *A decentralised control scheme*

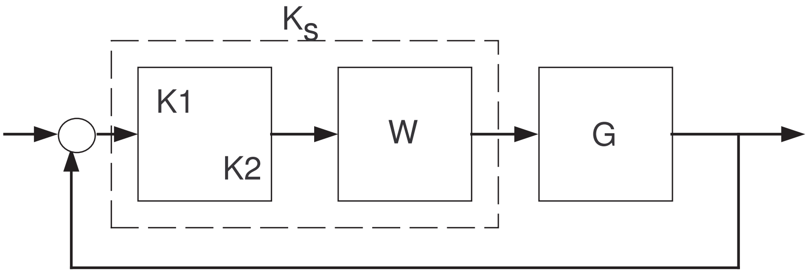

Figure 2: *A decentralised control scheme with decoupling precompensator W (s)*

to be diagonal at steady state condition (i.e. $G_s(0)$ is diagonal), then the decoupling is known as static decoupling. This can be done by using a precompensator of the form $W = G^{-1}(0)$. If the system is made to be almost diagonal at a required frequency ω_0 by using $W = G_0^{-1}$, where G_0 is the real approximation of $G(j\omega_0)$ then the system is approximately decoupled at the required frequencies.The bandwidth frequency is a good selection for ω_0 as the effect of performance of reducing interaction is maximum in this frequency. The limitations and detailed approach of decoupling a MIMO system is dealt with in [Skogestad and Postelwithe (2005)]. Some of the common strategies utilised in decoupling control are the internal model scheme and partial decoupling of upper or lower triangle of the transfer function matrix.
The control design for this system is to be done in two steps . The first step is to decouple the system G with a precompensator W as explained in Sec. 3.2.1. The next step is to design a controller K consisting of diagonal elements K_1, K_2,..., K_m for the decoupled SISO transfer function subsystems of G_s.

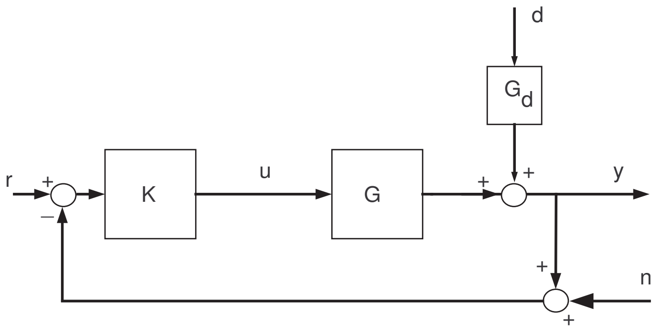

Figure 3: *Block diagram of one degree of freedom feedback controller*

3.2.2 Optimal Control Design

Generally for any system its output will be affected by unwanted noise or disturbances as shown in Fig. 3. Hence it is necessary that the controller we design suppresses the noise (disturbance rejection). The advantage of using Fig. 3 is that we can converge coloured noise signals into a white noise disturbance by including the noise dynamics in the system dynamics. In the case of wind turbines the wind speed variations within a time scale of 10 minutes is actually an unknown disturbance whose effects on the output needs to be suppressed. The most common methods of doing this is to derive a controller via an iteration scheme that minimises the 2 or ∞ norms of the transfer function between the error signal and the output. This will in turn minimise the effect of error signal on the output.

General problem formulation For a controller to be optimal the control problem needs to be generalised. For multivariable system this general problem formulation method that is followed in this report was introduced by Doyle [Doyle (1983)] as shown in Fig. 4. Consider the state space equation as given in Eq. 19

$$\begin{aligned} \dot{x}(t) &= \mathbf{A}x(t) + \mathbf{B}_1 w(t) + \mathbf{B}_2 u(t) \\ z(t) &= \mathbf{C}_1 x(t) + \mathbf{D}_{11} w(t) + \mathbf{D}_{12} u(t) \\ y(t) &= \mathbf{C}_2 x(t) + \mathbf{D}_{21} w(t) + \mathbf{D}_{22} u(t) \end{aligned} \tag{19}$$

where $w(t)$ is the generalised disturbance signal (A group of signals that affect the system and cannot be influenced by the controller). It consists of $d(t)$ which is the stochastic disturbance, $r(t)$ which is the set point signal and $n(t)$ which is the measurement noise. $z(t)$ is the signal that allows to characterize whether a controller has certain desired properties and is called controlled variable or performance variable. The ultimate goal is to reduce this signal to zero at all frequencies, but this is unrealistic due to actuation limits. $u(t)$ is the output signal of the controller and is called the control input and $y(t)$ is the measurement output. From the state space form described in Eq. 19 the general plant **P** can be described as given in Eq. 20

$$\begin{pmatrix} z \\ y \end{pmatrix} = \mathbf{P} \begin{pmatrix} w \\ u \end{pmatrix} = \begin{pmatrix} P_{11} & P_{12} \\ P_{21} & P_{22} \end{pmatrix} \begin{pmatrix} w \\ u \end{pmatrix} \tag{20}$$

where

$$\mathbf{P} = \left[\begin{array}{c|cc} \mathbf{A} & \mathbf{B}_1 & \mathbf{B}_2 \\ \hline \mathbf{C}_1 & \mathbf{D}_{11} & \mathbf{D}_{12} \\ \mathbf{C}_2 & \mathbf{D}_{21} & \mathbf{D}_{22} \end{array} \right] \tag{21}$$

The generalised plant can be described in terms of matrix transfer function **P** as shown in Fig. 4. It must be noted that **P** is called a generalized plant if there exists at least one controller **K** which stabilizes **P**. i.e $(\mathbf{A}\,\mathbf{B}_2)$ is at least stabilizable and $(\mathbf{A}\,\mathbf{C}_2)$ is detectable.
From Eq. 20 it is clear that

$$\begin{aligned} z &= P_{11}w + P_{12}u \\ y &= P_{21}w + P_{22}u \end{aligned} \tag{22}$$

The necessity of controller **K** is to reduce the deviation of controlled variable $z(t)$ with respect to the input variable $w(t)$. Hence absorbing the block **K** along with **P** we get the overall closed loop system **N** as shown in Fig. 5 with a representation

$$N = P_{11} + P_{12}K(I - P_{22}K)^{-1}P_{21} \triangleq F_l(P, K) \tag{23}$$

The above formulation of the control loop **N** is known as "lower linear fractional transformation"(LLFT). and is often given as follows

$$N \triangleq F_l(P, K) \tag{24}$$

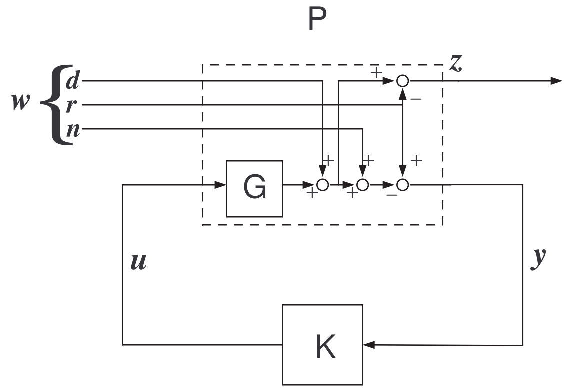

Figure 4: *Equivalent representation of Fig. 3*

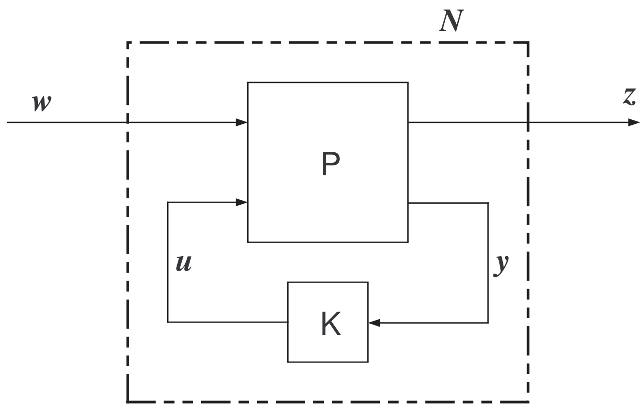

Figure 5: *General block diagram of closed loop system*

H_2 optimal control   The aim of H_2 optimal control problem is to find a stabilising controller **K** which minimizes the 2-norm cost function of the performance variable z(t) by reducing the 2 norm of the LLFT as follows

$$\|N(s)\|_2 = \sqrt{\int_{-\infty}^{\infty} tr\left[N(j\omega)N(j\omega)^H\right] d\omega} \tag{25}$$

The proof of how reducing the 2-norm cost function given in Eq. 25 reduces error is proven in [Skogestad and Postelwithe (2005)].
A special case of H_2 optimal control is the LQG problem . Consider a stochastic process

$$\begin{aligned} \dot{x} &= Ax + Bu + w_d \\ y &= Cx + w_n \end{aligned} \tag{26}$$

The LQG optimal control determines the stabilising controller **K** by reducing the 2- norm given in Eq. 25 but where the disturbance input to the closed loop system ω are gaussian white noise with unit intensity as shown in Eq. 27

$$Z \triangleq F_l(P, K)\omega(s) \tag{27}$$

H_∞ Control   Consider the general control configuration provided in Fig. 5. H_∞ control design , the other control design that uses the norm reduction method , designs a controller that reduces the ∞ norm of the transfer function between disturbance signal w(t) and the output z(t). In other words H_∞ control design tries to minimise the worst possible gain of the frequency responce at all frequencies of N(s). Hence the standard H_∞ problem is to find stabilizing controller K that minimizes

$$\|N(s)\|_\infty \quad = \max_{\omega} \bar{\sigma}(F_l(P,K)(j\omega)) \tag{28}$$

3.3 Controller Design choice and add ons

For Load reduction we need to design a multivariable controller that reduces the loads for wind speed disturbances. The choice of control technique depends on the fact that we need to reduce the 1P loads. To reduce the 1P load we need to reduce the load peaks at the 1P frequency. Hence the ideal choice is to reduce the 2-norm of the system ,in other words, implement the H_2 control technique. If we can model our system such that the input disturbance to the system is just gaussian white noise then we can utilise LQG control technique . But for disturbance rejection of colored noises a more useful technique is the feed forward control technique which can be added to the LQG controller.

3.3.1 Disturbance feed forward

This section will be discussed in discrete time as the control implementation of the feed forward control in this thesis will be in discrete time. A structure of feedforward control with measurable disturbance is given in Fig. 6.

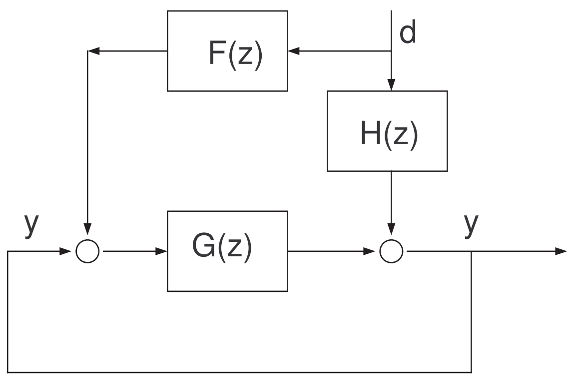

Figure 6: *Block diagram scheme for feed forward controller*

The controller F(z) is the feed forward controller for disturbance rejection. Consider the transfer function between y(k) and d(k).

$$y(k) = G(z)\cdot y(k) + G(z)\cdot F(z)\cdot d(k) + H(z)\cdot d(k) \tag{29}$$

$$y(k) = \frac{(G(z)\cdot F(z) + H(z))}{1-G(z)}\cdot d(k) \tag{30}$$

For ideal disturbance rejection the transfer function must be zero.Hence

$$0 = \frac{(G(z)\cdot F(z) + H(z))}{1-G(z)} \tag{31}$$

$$F(z) = -H(z)\cdot G(z)^{-1} \tag{32}$$

Here the feed forward block consists of the inverse of the state model G(z). Moreover the feed forward block transfer function F(z) must be stable and proper, because it acts in open loop. Hence it is necessary to make sure that $G(z)^{-1}$ is proper and stable. But it is possible that G(z) has zeros that cause non-minimum phase behaviour. In other words G(z) has zeros for $|z| > 1$. Hence we cannot invert G directly. Hence a novel method known as Stable Dynamic Inversion (SDI) technique [George et al. (1999)] is used. A brief overview of SDI technique is provided below.

Consider a non-minimum phase system given below

$$\begin{aligned} x(k+1) &= A \cdot x(k) + B \cdot u(k) + G \cdot w(k) \\ y(k) &= C \cdot x(k) + D \cdot u(k) + v(k) \end{aligned} \tag{33}$$

Let us consider the following model for our input signal u(k)

$$u(k+1) = u(k) + \eta(k) \tag{34}$$

for some $\eta(k)$. For simplicity we consider it to be white noise. Hence the augmented system becomes

$$\begin{aligned} x_a(k+1) &= A_a \cdot x_a(k) + G_a \cdot [w(k)'\eta(k)']' \\ y(k) &= C_a \cdot x(k) + H_a \cdot [v(k)'\eta(k)']' \end{aligned} \tag{35}$$

where

$$\begin{aligned} x_a(k) &= \begin{bmatrix} x(k) \\ u(k) \end{bmatrix} \\ A_a &= \begin{bmatrix} A & B \\ 0 & I \end{bmatrix} \end{aligned} \tag{36}$$

If (C,A) is observable and there is no zeros at z = 1 for the system Σ (A,B,C,D), then we can setup a kalman filter to estimate the input signal u(k). Then the stable inverse of the system Σ (A,B,C,D) is given by

$$\Sigma_{inv} = (0 \quad I)(zI - A_a + KC_a)^{-1}K \tag{37}$$

where K is the Kalman gain.

4 Feasibility study of simple control designs

In this chapter a feasibility study over multivariable controller design for a wind turbine is discussed. It is a known fact that a wind turbine is a MIMO (multi input multi output) system. But frequently you encounter systems where inputs and outputs can be grouped into pairs and treated as separate SISO (single input single output) sub systems that tend to form the MIMO system as is the case with the orthogonal tower moments (tilt and yaw).The tilt moment is an horizontal component whereas the yaw moment is a vertical component. Hence they are perpendicular to each other and hence orthogonal. All the literature on wind turbine control discussed in Sec. 2 utilise this fact to design simple SISO controllers. But, ever so often non negligible interactions between the multiple inputs and outputs can occur. Even though we consider that there is not much coupling between tilt and yaw moment of the wind turbine and consider them to be orthogonal, this is not totally true and there is some coupling between the two as will be shown by the TURBU model [van Engelen (2007)]. In such cases a multivariable control design is required in order to compensate for the coupling between the different scalar loops

4.1 Analysis of a simple wind turbine model

For the feasibility study of the various control design techniques, a simple linear model of a 2.5 MW 3-bladed wind turbine model as described in [van Engelen (2006)] is utilised . The model utilises stiff blades and stiff drive train. A controllable generator torque is included and stochastic wind speed excitation is utilised along with stationary aerodynamic conversion for derivation of flap and edge blade root moments. A schematic layout of the wind turbine model is pictured in Fig. 7.

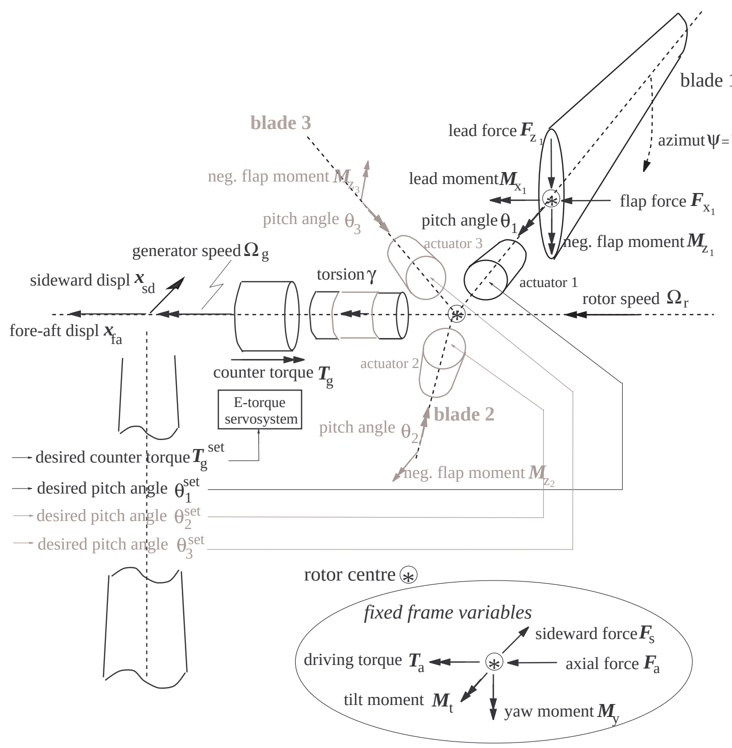

Figure 7: Schematic layout of wind turbine model. Courtesy: [van Engelen (2006)]

4.1.1 Linearised aerodynamic conversion

For the control model linear torque, force and moments need to be calculated. Linear BEM (Blade Element Momentum) theory is used for converting the aerodynamics which map the variations of the flap wise relative wind speed into blade moments (flap wise and lead wise blade root moments) and blade forces. To simplify the model unsteady aerodynamics and wake effects have not been taken into account. The aerodynamic conversions are based on converting relative flap wise wind speed v_{fl_i} into flap and lead wise blade root moments and forces (aerodynamic gains). These moments and forces for pitch angle variations θ_i and relative velocity v_{fl_i} of the i^{th} blade is characterised as given in Eq. 38

$$\begin{array}{rclcll} \delta M_{z,i} &=& h_{M_z} v_{fl_i} &+& k_{M_z}\theta_i & \text{(neg.flapwise moment)} \\ \delta F_{x,i} &=& h_{F_x} v_{fl_i} &+& k_{F_x}\theta_i & \text{(pos.flapwise force)} \\ \delta M_{x,i} &=& h_{M_x} v_{fl_i} &+& k_{M_x}\theta_i & \text{(pos.flagwise moment)} \\ \delta F_{z,i} &=& h_{F_z} v_{fl_i} &+& k_{F_z}\theta_i & \text{(pos.flagwise force)} \end{array} \tag{38}$$

From these aerodynamic gains, the variations in driving torque δT_a, in axial force δF_a, in the tilt moment δM_t and in the sidewards force are given by Eq. 39

$$\begin{array}{rcl c rcl} \delta T_a &=& \sum_{i=1}^{B} \delta M_{x,i} &;& \delta F_a &=& \sum_{i=1}^{B} \delta F_{x,i} \\ \delta M_t &=& \sum_{i=1}^{B} \sin\psi_i \, \delta M_{z,i} &;& \delta F_s &=& \sum_{i=1}^{B} \sin\psi_i \, \delta F_{z,i} \end{array} \tag{39}$$

The flapwise relative wind speed variation v_{fl_i} for the i^{th} blade is the sum of the blade effective wind speed $\tilde{u}_i$ and the upwind motion of the rotor blade. The latter is caused by fore-aft tower bending only since rigid blades are assumed. The upwind structural motion involves both the fore-aft translation x_{fa} and tilt rotation $\dot{\phi}_{fa}$ of the tower top. The latter has an azimuth dependent effect on the relative wind speed which varies over the rotor radius. The 3/4 blade radius location of the rotor blades ($\frac{3R_b}{4}$) is assumed to be the effective location for taking into account $\dot{\phi}_{fa}$ in the one-point-model-approach to blade loading. The flapwise relative wind speed v_{fl_i} is determined as:

$$v_{fl_i} = \tilde{u}_i - \dot{x}_{fa} + \sin(\psi_i)\frac{3}{2H}\frac{3R_b}{4}\dot{x}_{fa} \tag{40}$$

The multiplier 3/2H is exactly the ratio between displacement and rotation if a prismatic beam of length H is subjected to a bending force load. At azimuth angle ψ equal to 0, the first blade is in the horizontal position while it is rotating downward. For the azimuth angles ψ_1, ψ_2, ψ_3 of the three blades holds:

$$\psi_1 = \psi \quad ; \psi_2 = \psi + \frac{2\pi}{3} \quad ; \psi_3 = \psi + \frac{4\pi}{3} \tag{41}$$

The gains h_{M_z} . . . k_{F_z} are derived from the power and thrust coefficient data in a chosen working point, characterised by wind speed, rotor speed and pitch angle. The derivation is constrained by the assumption of equal aerodynamic efficiency along the blade radius, which implies a linear increasing flapwise force per unit span $f_{fl}(r)$ over the rotor radius and constant leadwise force per unit span $f_{ld}(r)$.

4.1.2 Periodic linear model equations

The model equations required for controller design are the basic equations of motion of the tower and rotor and the output equations of the blade moments caused by the wind disturbances.

Equations of motion The drive train is accelerated by the aerodynamic driving torque T_a and decelerated by the generator torque T_g. Hence the rotor speed Ω is a function of the two torques.

$$J \cdot \dot{\Omega} = \delta T_a - \delta T_g \tag{42}$$

with linearised torque variation δT_a from Eqs. 38,39 and 40 is given by

$$\delta T_a \quad = \quad \sum_{i=1}^{B}[h_{M_x}\tilde{u}_i + k_{M_x}\theta_i] \quad - \quad Bh_{M_x}\dot{x}_{fa} \tag{43}$$

The variables of the included tower model are the fore-aft and the sidewards displacements x_{fa} and x_{sd} respectively. The fore-aft motion is driven by the aerodynamic thrust force F_a and the tilt moment M_t. The sidewards motion is generated by the generator torque T_g and the sidewards aerodynamic force F_s.

$$\begin{array}{rcl} m_{tw}\,\ddot{x}_{fa} & = & \delta F_a + \frac{3}{2H}\,\delta M_t - s_{tw}x_{fa} - d_{tw}\dot{x}_{fa} \\ m_{tw}\,\ddot{x}_{sd} & = & \frac{3}{2H}\,\delta T_g + \delta F_s - s_{tw}x_{sd} - d_{tw}\dot{x}_{sd} \end{array} \tag{44}$$

The multiplication factor $\frac{3}{2H}$ for the bending moment loads in the equations of motion applies for the prismatic beam. For the linearised variation in the axial force, tilt moment and sideward force holds(Eq. 39; $\sum_{i=1}^{B}\sin^2\psi_i = \frac{1}{2}B$)

$$\begin{array}{rcl} \delta F_a & = & \sum_{i=1}^{B}[h_{F_x}\tilde{u}_i + k_{F_z}\theta_i] - Bh_{F_x}\dot{x}_{fa} \\ \delta M_t & = & \sum_{i=1}^{B}\sin\psi_i[h_{M_z}\tilde{u}_i + k_{M_z}\theta_i] + \frac{3}{2}\frac{9R_b}{8H}h_{M_z}\dot{x}_{fa} \\ \delta F_s & = & \sum_{i=1}^{B}-\sin\psi_i[h_{F_z}\tilde{u}_i + k_{F_z}\theta_i] - \frac{3}{2}\frac{9R_b}{8H}h_{F_z}\dot{x}_{fa} \end{array} \tag{45}$$

The values of tower top equivalent mass m_{tw}, spring constant $s_{tw}$and damper constant d_{tw} are based on following structural data

- horizontal tower displacement at unity force.
- damping rate of the first bending mode.
- average of the first fore-aft and sidewards frequency.

Output equations For feedback control, along with equations of motion, we also need to consider output equations. Individual pitch control is used to reduce bending moments. Hence it is only logical that we choose the feedback of blade root bending moment variations $\delta M_{z,i}$ for the control problem.

$$\delta M_{z_1} \quad = \quad -h_{M_z}(1-\sin\psi_1\frac{9R_b}{8H})\dot{x}_{fa} + h_{M_z}\tilde{u}_1 + k_{M_z}\theta_1 \tag{46}$$

$$\delta M_{z_2} \quad = \quad -h_{M_z}(1-\sin\psi_2\frac{9R_b}{8H})\dot{x}_{fa} + h_{M_z}\tilde{u}_2 + k_{M_z}\theta_2 \tag{47}$$

$$\delta M_{z_3} \quad = \quad -h_{M_z}(1-\sin\psi_3\frac{9R_b}{8H})\dot{x}_{fa} + h_{M_z}\tilde{u}_3 + k_{M_z}\theta_3 \tag{48}$$

4.1.3 Azimuth dependency and Coleman Transformation

It can be clearly seen by substituting Eqs. 38, 39 and 40 in Eqs. 42 and 44 that the states of the tower and the blade moments are azimuth dependant as follows

$$
\begin{aligned}
J \cdot \dot{\Omega} &= \sum_{i=1}^{B} [h_{M_z} \tilde{u}_i + k_{M_x} \theta_i] - B h_{M_x} \dot{x}_{fa} - \delta T_g && (49)\\
m_{tw}\, \ddot{x}_{fa} &= \sum_{i=1}^{B} [h_{F_x} \tilde{u}_i + k_{F_z} \theta_i] - B h_{F_x} \dot{x}_{fa} + \frac{3}{2H} \sum_{i=1}^{B} \sin\psi_i [h_{M_z} \tilde{u}_i + k_{M_z} \theta_i] && (50)\\
&\quad + \frac{3}{2H} \frac{27 R_b}{16} h_{M_z} \dot{x}_{fa} - s_{tw} x_{fa} - d_{tw} \dot{x}_{fa} \\
m_{tw}\, \ddot{x}_{sd} &= \frac{3}{2H}\, \delta T_g\ + \sum_{i=1}^{B} - \sin\psi_i [h_{F_z} \tilde{u}_i + k_{F_z} \theta_i] - \frac{3}{2H} \frac{27 R_b}{16} h_{F_z} \dot{x}_{fa} && (51)\\
&\quad - s_{tw} x_{sd} - d_{tw} \dot{x}_{sd}
\end{aligned}
$$

To enable linear control design, the periodic coefficients in these equations are eliminated by formulating the structural and aerodynamic degrees of freedom (DOF) for the rotor in multi-blade coordinates (using Coleman transform).

The multi-blade transformation or Coleman transformation [Coleman and Feingold (1958)] for rotor blades is a transformation which maps the individual blade coordinates present in the periodic frame of reference into a fixed frame of reference. In other words the Coleman transformation maps the rotor coordinates with the tower coordinates. In due process the periodic terms of the aero-elastic equations will be eliminated, as the number of blades is odd meaning the rotor is isotropic (identical and symmetrically mounted blades), and the inflow to the rotor is uniform.

The periodic terms are eliminated by multiblade transformation, because the coordinates of the model are defined in the same frame of reference as explained in [Hansen (2003)]. For example the physical coordinate q_i for blade i in the rotating frame will be converted by Coleman transform as follows

$$
q_i(t) = q_1^{cm}(t) + q_3^{cm}(t) \cos\left(\psi t + \frac{2\pi}{3}(i-1)\right) + q_2^{cm}(t) \sin\left(\psi t + \frac{2\pi}{3}(i-1)\right) \tag{52}
$$

where t is time, and ψ is the azimuth angle of the rotor. The three multiblade coordinates q_1^{cm}, q_2^{cm} and q_3^{cm} replace the blade coordinates q_1, q_2 and q_3. For example we can map the blade variable 'the blade pitch angles θ_i'into 'fixed coordinate system'(superscript^{cm}) as given in Eq. 53

$$
\begin{bmatrix} \theta_1(t) \\ \theta_2(t) \\ \theta_3(t) \end{bmatrix} = \begin{pmatrix} 1 & \sin\psi_1(t) & \cos\psi_1(t) \\ 1 & \sin\psi_2(t) & \cos\psi_2(t) \\ 1 & \sin\psi_3(t) & \cos\psi_3(t) \end{pmatrix} \cdot \begin{bmatrix} \theta_1^{cm}(t) \\ \theta_2^{cm}(t) \\ \theta_3^{cm}(t) \end{bmatrix} \tag{53}
$$

Similarly we can also convert the fixed coordinates into the rotating frame of reference using inverse Coleman transform as done for deriving the blade loads

$$
\begin{bmatrix} M_{z_1}^{cm}(t) \\ M_{z_2}^{cm}(t) \\ M_{z_3}^{cm}(t) \end{bmatrix} = \begin{pmatrix} \frac{1}{3} & \frac{1}{3} & \frac{1}{3} \\ \frac{2}{3}\sin\psi_1(t) & \frac{2}{3}\sin\psi_2(t) & \frac{2}{3}\sin\psi_3(t) \\ \frac{2}{3}\cos\psi_1(t) & \frac{2}{3}\cos\psi_2(t) & \frac{2}{3}\cos\psi_3(t) \end{pmatrix} \cdot \begin{bmatrix} M_{z_1}(t) \\ M_{z_2}(t) \\ M_{z_3}(t) \end{bmatrix} \tag{54}
$$

where $M_{z,i}$ and $\psi_i(t)$ are the blade flap moments and the azimuth angles of blade *i* respectively.
It is assumed that uncoupled transfer functions can be derived for the rotor speed $\Omega(t)$ and tilt- and yaw wise multiblade coordinates ${M_{z_2}}^{cm}(t)$ and ${M_{z_3}}^{cm}(t)$ of the flapwise moments from this design model. Hence a LTI scalar control design could be implemented for each multi blade coordinate angle ${\theta_i}^{cm}(t)$.

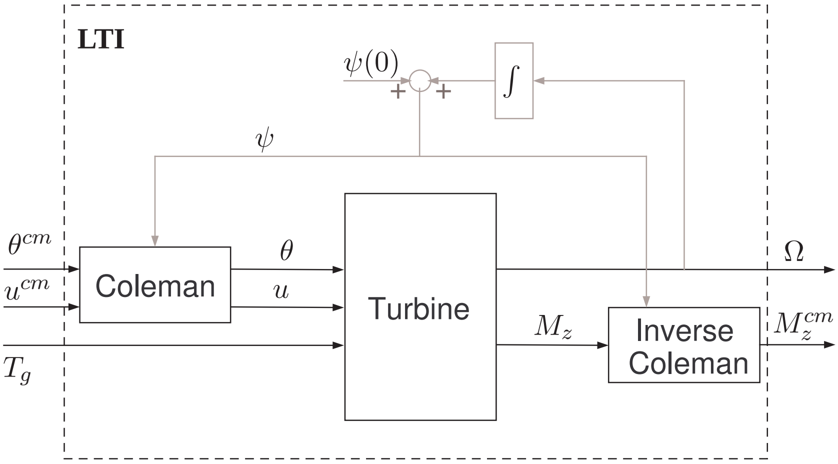

Figure 8: Conversion of periodic model into linear model using Coleman transformation

4.1.4 Linear time invariant model

The equations of motion that depend on the azimuth angle (ψ) do not include state variables attached to the rotor blade and rotor shaft except the rotational speed Ω (x_{fa} and x_{sd}, the other two state variables are attached to the tower). Since Ω has a co-axial orientation, not any state variable needs to be transformed or in other words the Coleman transformation has no affect on the state variables. The flap wise bending moments, pitch angles and blade effective wind speeds are the variables that need to be transformed. This transformation is done using the Coleman transformation matrix **P**. The Coleman transformation matrix **P** maps the multi-blade coordinates p_{cm} to rotating coordinates p. The second and third multi blade flap moment coordinates δM_{tilt} and δM_{yaw} have tilt and yaw orientation.

$$
\begin{aligned}
J \cdot \dot{\Omega} &= -3h_{M_x}\dot{x}_{fa} + 3k_{M_x}\theta_1^{cm} + 3h_{M_x}\tilde{u}_1^{cm} - \delta T_g && (55)\\
m_{tw}\,\ddot{x}_{fa} &= -s_{tw}x_{fa} - (d_{tw} + 3h_{F_x} - \frac{81R_b}{32H^2}h_{M_z})\dot{x}_{fa} + 3k_{F_x}\theta_1^{cm} && (56)\\
&\quad + \frac{9}{4H}k_{M_z}\theta_2^{cm} + 3h_{F_x}\tilde{u}_1^{cm} + \frac{9}{4H}h_{M_z}\tilde{u}_2^{cm} && (57)\\
m_{tw}\,\ddot{x}_{sd} &= \frac{3}{2H}\delta T_g - \frac{27R_b}{16H}h_{F_z}\dot{x}_{fa} - \frac{3}{2}k_{F_z}\theta_2^{cm} - \frac{3}{2}h_{F_z}\tilde{u}_2^{cm} - s_{tw}x_{sd} - d_{tw}\dot{x}_{sd} && (58)
\end{aligned}
$$

and

$$
\begin{aligned}
\delta M_{z_{cm1}} &= -h_{M_z}\dot{x}_{fa} + k_{M_z}\theta_1^{cm} + h_{M_z}\tilde{u}_1^{cm} && (59)\\
\delta M_{tilt} &= -h_{M_z}\frac{27R_b}{16H}\dot{x}_{fa} - \frac{3}{2}k_{M_z}\theta_2^{cm} - \frac{3}{2}h_{M_z}\tilde{u}_2^{cm} && (60)\\
\delta M_{yaw} &= \frac{3}{2}k_{M_z}\theta_3^{cm} + \frac{3}{2}h_{M_z}\tilde{u}_3^{cm} && (61)
\end{aligned}
$$

For control purposes this system is written in state space form and then discretized with a sampling time of 0.02 sec.

$$\begin{aligned}
\begin{bmatrix} \dot{\Omega} \\ \dot{x}_{fa} \\ \ddot{x}_{fa} \\ \dot{x}_{sd} \\ \ddot{x}_{sd} \end{bmatrix} &= \begin{bmatrix} 0 & 0 & \frac{-3h_{M_x}}{J} & 0 & 0 \\ 0 & 0 & 1 & 0 & 0 \\ 0 & -\frac{s_{tw}}{m_{tw}} & -\frac{(d_{tw}+3h_(F_x)-\frac{81r_b}{32H^2}h_{M_z})}{m_{tw}} & 0 & 0 \\ 0 & 0 & 0 & 0 & 1 \\ 0 & 0 & -\frac{\frac{27R_b}{16H}h_{F_z}}{m_{tw}} & -\frac{s_{tw}}{m_{tw}} & -\frac{d_{tw}}{m_{tw}} \end{bmatrix} \begin{bmatrix} \Omega \\ x_{fa} \\ \dot{x}_{fa} \\ x_{sd} \\ \dot{x}_{sd} \end{bmatrix} \\
&+ \begin{bmatrix} \frac{3h_{M_x}}{J} & 0 & 0 & \frac{3k_{M_x}}{J} & 0 & 0 & -\frac{1}{J} \\ 0 & 0 & 0 & 0 & 0 & 0 & 0 \\ \frac{3h_{F_x}}{m_{tw}} & \frac{\frac{9}{4H}h_{M_z}}{m_{tw}} & 0 & \frac{3k_{F_x}}{m_{tw}} & \frac{\frac{9}{4H}k_{M_z}}{m_{tw}} & 0 & 0 \\ 0 & 0 & 0 & 0 & 0 & 0 & 0 \\ 0 & -\frac{\frac{3}{2}h_{F_z}}{m_{tw}} & 0 & 0 & -\frac{\frac{3}{2}k_{F_z}}{m_{tw}} & 0 & \frac{\frac{3}{2H}}{m_{tw}} \end{bmatrix} \begin{bmatrix} \tilde{u}_1^{cm} \\ \tilde{u}_2^{cm} \\ \tilde{u}_1^{cm} \\ \theta_1^{cm} \\ \theta_2^{cm} \\ \theta_3^{cm} \\ \delta T_g \end{bmatrix}
\end{aligned} \tag{62}$$

$$\begin{aligned}
\begin{bmatrix} \Omega \\ \delta M_{z_{cm1}} \\ \delta M_{tilt} \\ \delta M_{yaw} \end{bmatrix} &= \begin{bmatrix} 1 & 0 & 0 & 0 & 0 \\ 0 & 0 & -h_{M_z} & 0 & 0 \\ 0 & 0 & -\frac{27R_b}{16H}h_{M_z} & 0 & 0 \\ 0 & 0 & 0 & 0 & 0 \end{bmatrix} \begin{bmatrix} \Omega \\ x_{fa} \\ \dot{x}_{fa} \\ x_{sd} \\ \dot{x}_{sd} \end{bmatrix} \\
&+ \begin{bmatrix} 0 & 0 & 0 & 0 & 0 & 0 & 0 \\ h_{M_z} & 0 & 0 & k_{M_z} & 0 & 0 & 0 \\ 0 & -\frac{3}{2}h_{M_z} & 0 & 0 & -\frac{3}{2}k_{M_z} & 0 & 0 \\ 0 & 0 & \frac{3}{2}h_{M_z} & 0 & 0 & \frac{3}{2}k_{M_z} & 0 \end{bmatrix} \begin{bmatrix} \tilde{u}_1^{cm} \\ \tilde{u}_2^{cm} \\ \tilde{u}_1^{cm} \\ \theta_1^{cm} \\ \theta_2^{cm} \\ \theta_3^{cm} \\ \delta T_g \end{bmatrix}
\end{aligned} \tag{63}$$

4.2 Multivariable Control

From Eq. 63 it is clear the outputs of the system (the loads) that we need to reduce depend on the states ($\dot{x}_{fa}$), known inputs in pitch angles (θ_i) and unknown coloured disturbances in wind speed ($\tilde{u}_i^{cm}$). Hence for optimal load reduction we also need to model the unknown coloured disturbances. But using the standard multivariable techniques it is not possible to determine optimal feedback gain for load reduction caused by coloured disturbances. Hence we need to define a model for the unknown wind inputs which would generate the Coleman winds from white noise input. It can be done in two ways.

- Identify a wind model based on wind signal measurements or blade effective simulated wind signals.
- Use a random walk model that will map the low order behavior of the wind signal

For identification purposes blade effective wind signal samples were used to generate a sixth state identification model. The blade effective wind signals were converted to Coleman wind signals and were then utilised for identification. The model was identified using PO-MOESP identification technique [Verhaegen and Verdult (2005)] with white noise inputs and Coleman wind signal outputs. The frequency response of the identified model is shown in Fig. 9. The first row shows the frequency response of the first Coleman mode to the three input white noise signals. The second row is the frequency response for the second Coleman mode wind signal and the third row for the third Coleman mode signal respectively, with the input signals being white noises.

For individual pitch control we require to compensate only the tilt and yaw moments as they cause the asymetric loads on the tower. Hence for load reduction we need only Coleman mode wind inputs

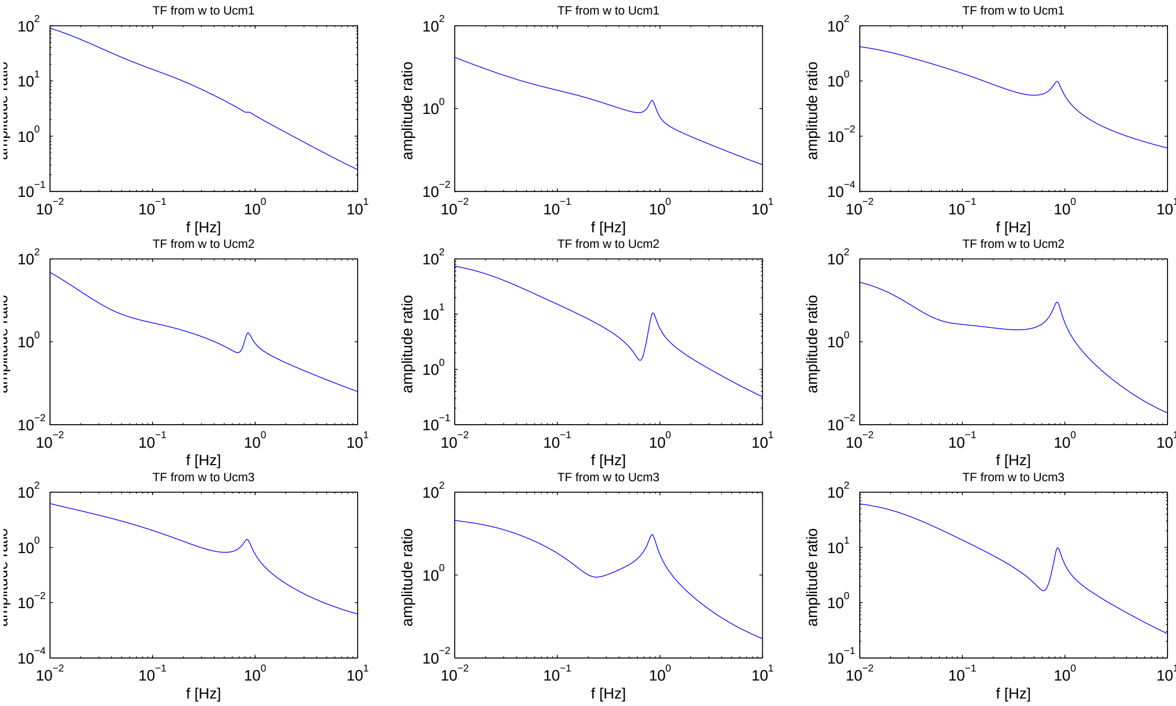

Figure 9: frequency response of the Identified wind model with white noise input and Coleman wind output

U_2^{cm} and U_3^{cm} which are the wind components in the horizontal and vertical directions. The 0P and 1P frequency of the wind turbine (Coleman domain) is essentially at around 0 Hz to 0.3 Hz (The 1P and 2P frequencies of the rotor blade are converted into 0P and 3P frequencies of the Coleman domain respectively. Generally speaking 0P frequency of the Coleman domain is enough for the present work, but 1P frequency is also included here just to show that the random walk model is sufficient higher harmonic control as well). Moreover the limitations posed by the pitch actuator on high frequency wind signals means that we need not concern ourselves with frequencies higher than 1 Hz. Hence we need a wind model that has the same spectrum of the wind signals upto that frequency. A random walk model can be used for such purposes as the spectrum of the random walk model will be similar to that of the wind spectrum at such low frequencies as shown by Fig. 10[1].

In this thesis the random walk model is utilised to generate the wind model for the following reasons.

- Random walk models are a tried and tested method of modeling bias and has been utilised in design of unknown wind inputs before [Mesic et al. (2003)].
- At 1P frequency the spectrum of the wind is generally an integrator slope. Hence we need not identify high order models based on wind measurements or blade effective wind signals.
- Random walk model is the simplest model for representing for stationary processes. The proof of stationarity of the Coleman wind input is provided in Sec. A.1

Furthermore the PSD of the two models and the measured signal shows that random walk model is an appropriate choice for wind estimation as shown in Fig. 11

A brief description of a random walk process and how an augmented wind turbine model containing wind model can be generated is explained below.

[1] To compensate for the tilt and yaw moments we need only the second and third Coleman domain wind signals as can be seen from Eqns 60 and 61. Hence the random walk model is derived only for these two wind signals

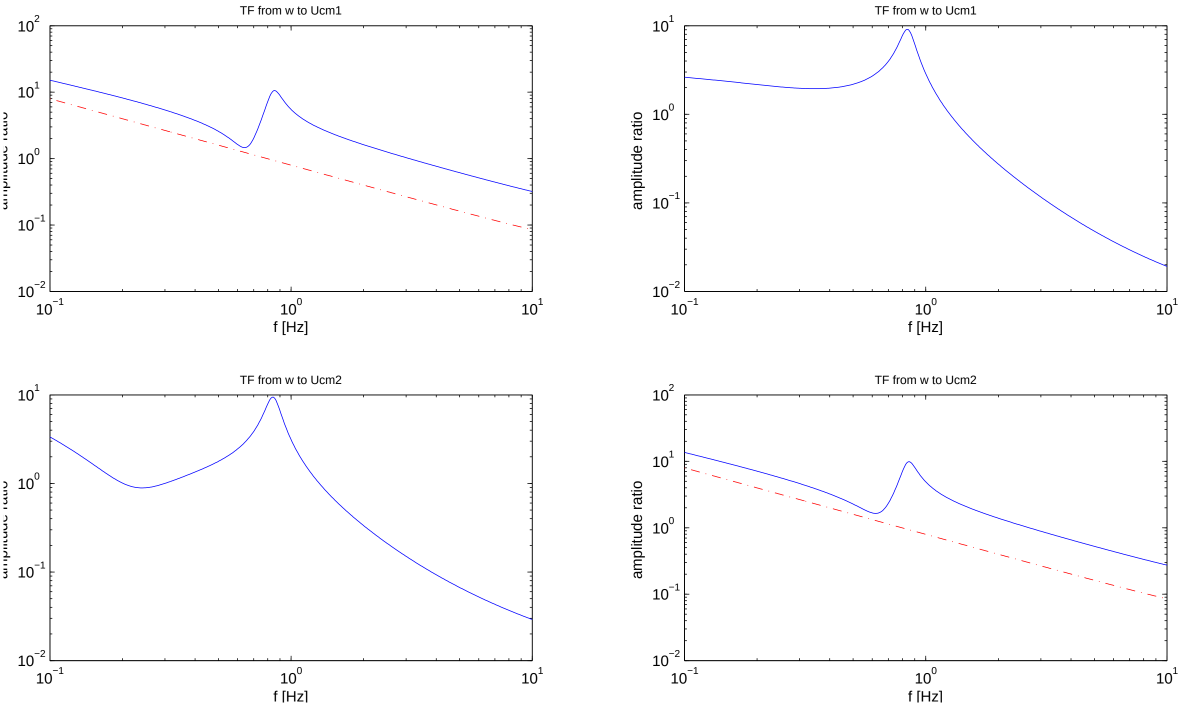

Figure 10: frequency response of the Identified wind model (blue) and random walk model (red dashed) with white noise input and Coleman wind outputs ($U_2^{cm} and U_3^{cm}$)

4.2.1 Random walk process

A random walk is a simple type of discrete stochastic process whose increments form a white noise. Since a white noise has zero mean, a random walk also has zero mean. A discrete univariate stochastic process R is called a random walk if its increments form a white noise.

$$W(k) = R(k) - R(k-1) \tag{64}$$

Because there are different types of white noises, there are different types of random walks. A simple random walk is one whose increments form a strong white noise whose terms only take on the values 1 or Ű1, each with probability 0.5. an arithmetic random walk is a random walk with increments that are a Gaussian white noise. This can be represented as

$$R(k) - R(k-1) = \sigma N(k) \tag{65}$$

where the N (k) are independent and identically distributed standard normal random variables, and σ is a constant. If a constant drift term μ is added, this becomes an arithmetic random walk with drift.

$$R(k) - R(k-1) = \mu + \sigma N(k) \tag{66}$$

For the wind model we assume that there is no drift involved in the system and hence utilise the simple random walk model.

$$R(k) = R(k-1) + Q_z w(k-1) \tag{67}$$

where Q_z is the covariance matrix for the white noise.

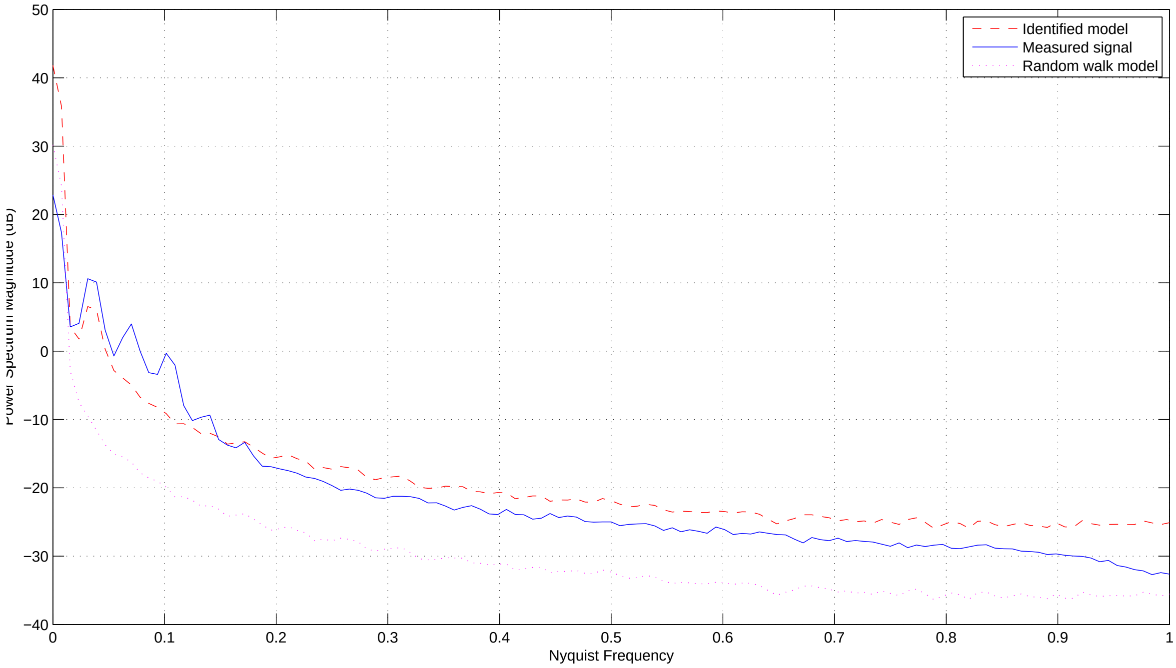

Figure 11: PSD of measured wind signal (blue solid), PSD of the identified model (red dashed), and PSD of the random walk model (Magenta dotted) all for wind signal Ucm2

4.2.2 Estimation of turbine model using random walk technique

The wind turbine model has two known inputs (θ_2^{cm} and θ_3^{cm}) and two unknown inputs (u_2^{cm} and u_3^{cm}). Lets consider the state space model of the wind turbine given in Eq. 68

$$\begin{aligned} x^{wt}(k+1) &= A_{wt}x^{wt}(k) + B_{wt}^{\theta}\theta_{cm}(k) + B_{wt}^{u}u_{cm}(k) + w(k) \\ y^{wt}(k) &= C_{wt}x^{wt}(k) + D_{wt}^{\theta}\theta_{cm}(k) + D_{wt}^{u}u_{cm}(k) + v(k) \end{aligned} \tag{68}$$

where u_{cm} are the unknown inputs with a known matrix B_{wt}^{u}. Many stochastic processes can be generated by driving linear systems with white noise sequences. Assume the following model representation for the unknown input wind signals, which is a general state space formulation of a random walk process.

$$\begin{aligned} z(k+1) &= \Phi z(k) + w_z(k) \\ u_{cm}(k) &= \Gamma z(k) \end{aligned} \tag{69}$$

To generate the random walk model $u_{cm}(k) = u_{cm}(k-1) + w_z(k-1)$ from the general state space formulation for wind signals given in Eq. 69 we take Φ and Γ as identity matrices with a covariance matrix Q_z of 0.1. The reason for this is that this generates the simplest random walk model and is basically an integrator model with a similar slope to that of the identified model as shown in Fig. 10 and also the PSD for this model is similar to that of the measured signal at 1P frequency Fig. 11. The combination of Eq. 68 and Eq. 69 results in an augmented state space system that denotes the total wind turbine system

$$\begin{aligned} \begin{bmatrix} x^{wt}(k+1) \\ z(k+1) \end{bmatrix} &= \begin{bmatrix} A_{wt} & B_{wt}^{u}\Gamma \\ 0 & \Phi \end{bmatrix} \begin{bmatrix} x^{wt}(k) \\ z(k) \end{bmatrix} + \begin{bmatrix} B^{\theta}wt \\ 0 \end{bmatrix} \theta_{cm}(k) + \begin{bmatrix} w(k) \\ w_z(k) \end{bmatrix} \\ y^{wt}(k) &= \begin{bmatrix} C_{wt} & 0 \end{bmatrix} \begin{bmatrix} x^{wt}(k) \\ z(k) \end{bmatrix} + \begin{bmatrix} D_{wt}^{\theta} \\ 0 \end{bmatrix} \theta_{cm}(k) + v(k) \end{aligned} \tag{70}$$

A Kalman filter is used to estimate $x^{wt}(k)$ and $z(k)$. The estimated unknown signal $\tilde{u}_c m(k)$ can further be obtained by Eq. 69 from the estimated state $\tilde{z}(k)$. Robustness issues of the random walk model is explained in detail in [Mesic et al. (2003)]. The necessary condition for accurate reconstruction of the states of the augmented system via Kalman filter is the observability of the system. The proof for observability of the augmented system containing the random walk model is given in appendix A.2

4.2.3 Determination of feedback gain

It can be proved using Popov-Belevitch-Hautus (PBH) test that the system given in Eq. 70 is observable [Mesic et al. (2003)]. Thus the Kalman filter to determine an unbiased estimate of the wind turbine along with the wind can be determined from the Kalman filter. The augmented system in Eq. 70 is observable but not controllable as the system also includes the wind states which are located in the uncontrollable subspace. Moreover since we use a random walk model this subspace is also not stabilizable. Hence the control gain for the augmented wind turbine is found in a two fold manner. The wind turbine subsystem that is responsible for blade loads can be given by two transfer functions. One relating to the blade loads caused by the pitch angle and the other one related to the wind disturbance as given by Fig. 12.

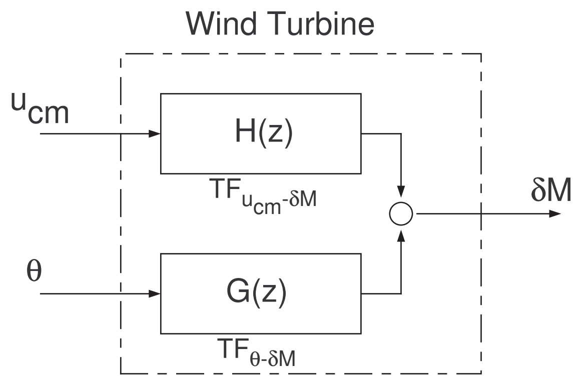

Figure 12: *Block diagram scheme for the wind turbine transfer functions related to Coleman moments*

Optimal gain for wind turbine states   Consider the transfer function between the pitch angle and the moments. In state space form it is given as follows [2].

$$\begin{aligned} x^{wt}(k+1) &= A_{wt}x^{wt}(k) + B^{\theta}_{wt}\theta_{cm}(k) + w(k) \\ y^{wt}(k) &= C_{wt}x^{wt}(k) + D^{\theta}_{wt}\theta_{cm}(k) + v(k) \end{aligned} \tag{71}$$

the feedback gain for the load reduction is determined by using the feedback law $\theta_{cm}(k)$ = - K x(k) that minimizes the cost function

$$J = \sum_{k=0}^{\infty} x(k)^{wt^T} Q x(k)^{wt} + \theta_{cm}(k)^T R \theta_{cm}(k) \tag{72}$$

[2]Here we consider that the wind speed has no effect on the states of the wind turbine. The reason being the effect of the states due to wind speed will be compensated by a feed forward controller as explained later.

Pseudo feed forward wind disturbance rejection   Feed forward mechanism is utilised for disturbance rejection or in other words to reduce the load caused by wind disturbance. Actually we do not measure wind speed but based on the assumption that the Kalman filter, given in Sec. 4.2.2, provides us with an unbiased estimate of the wind speed we can design a feed forward controller for wind speed feed forward rejection. Consider Fig. 13, the controller (F(z)) is the feed forward controller that reduces the load caused by wind disturbance as given in Sec. 3.3.1

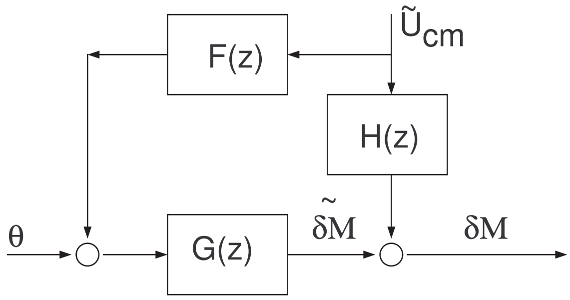

Figure 13: *Block diagram scheme for feed forward controller*

The gain for load reduction of the blade moments caused by wind disturbance can then be determined as follows. Consider the wind turbine model given in Eq. 68 and Eq. 63. On closer examination it can be seen that the influence of $\tilde{u}_2^{cm}$ and $\tilde{u}_3^{cm}$ have minimal effect on the states of the system. Moreover the tilt and yaw moments are decoupled. Thus changing the effect of the second and third Coleman domain winds will not affect the states of the system. Thus the dynamic feed forward control action for disturbance rejection is only a static gain for our simple model.
As the yaw component as no effect on the states of the wind turbine the feed forward gain required for compensation is just a static gain which simplifies the design of the controller. Hence the feed forward gains required for the compensation of the tilt moment caused by the wind disturbance is calculated as follows

$$\delta M_{tilt} = -h_{M_z}\frac{27R_b}{16H}\dot{x}_{fa} - \frac{3}{2}k_{M_z}\theta_2^{cm} - \frac{3}{2}h_{M_z}\tilde{u}_2^{cm} \tag{73}$$

But for the feed forward controller the load caused by the wind disturbance is the one that needs to be compensated . Hence the ideal feed forward gain would minimize the δM_{tilt} (caused by $\tilde{u}_2^{cm}$) to zero. Hence

$$\begin{aligned} 0 &= -\frac{3}{2}k_{M_z}\theta_2^{cm} - \frac{3}{2}h_{M_z}\tilde{u}_2^{cm} && (74)\\ \theta_2^{cm} &= -\frac{\frac{3}{2}h_{M_z}}{\frac{3}{2}k_{M_z}}\tilde{u}_2^{cm} && (75)\\ \theta_2^{cm} &= -\frac{h_{M_z}}{k_{M_z}}\tilde{u}_2^{cm} && (76)\end{aligned}$$

A similar approach is used to calculate the feed forward gain for yaw moment (δM_{yaw}). From Eq. 61 we know that the yaw moment depends on the yaw component of the pitch angle and the wind. Hence

$$\begin{aligned} 0 &= \frac{3}{2}k_{M_z}\theta_3^{cm} + \frac{3}{2}h_{M_z}\tilde{u}_3^{cm} && (77)\\ \theta_3^{cm} &= -\frac{h_{M_z}}{k_{M_z}}\tilde{u}_3^{cm} && (78)\end{aligned}$$

4.2.4 Controller design

The Kalman filter provides an unbiased estimate of the wind speed and hence the feed forward gain added to the state feedback gain is optimal. The controller is designed as given in Fig. 14

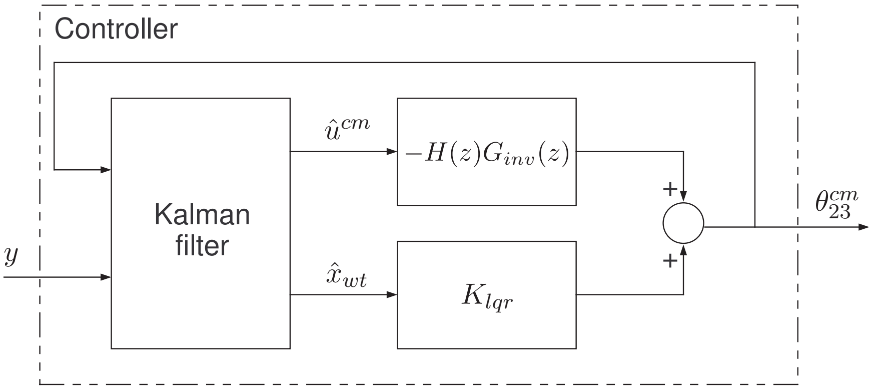

Figure 14: The complete feedback-feedforward control scheme

4.3 Feedback law

The overall layout of the feedback loops for rotor speed regulation and blade load reduction is pictured in Fig. 16. The feedback loop maps

- The low pass filtered rotational speed $\Omega_g$to the collective pitch angle set point θ_{col}^{pow}via a PI compensator, enforced by a feed forward of the estimated wind speed while catering for dynamic inflow effects.

- Identically low pass filtered tilt- and yaw- oriented multi-blade flap moment coordinates $\delta M_{z_{cm2}}$ and$\delta M_{z_{cm3}}$ to the tilt- and yaw- oriented multi-blade pitch angle coordinates θ_2^{cm} and θ_3^{cm} via LQG controller designed using Kalman filter (Sec. 4.2.2) and optimal gain (Sec. 4.2.3) described above.

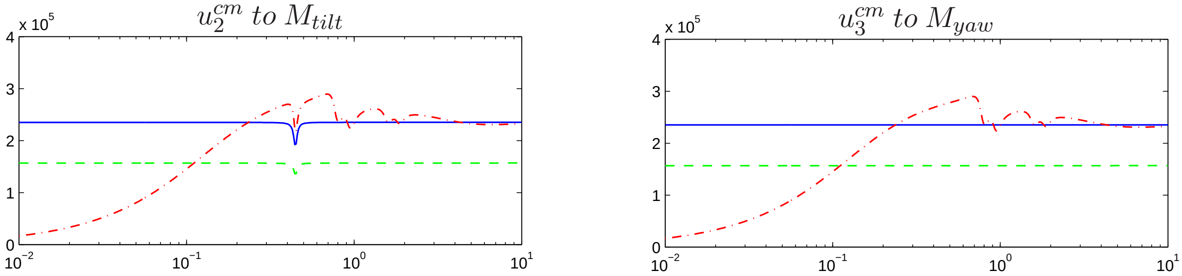

Figure 15: Frequency response plot of tilt moment M_{tilt} (first row) and yaw moment M_{yaw} (second row) due to the multi-blade wind inputs u_2^{cm} (left column) and u_3^{cm} (right column) for the simple rigid turbine model with no IPC (blue solid), conventional IPC (red dash-dotted) and new feedback-feedforward IPC (green dashed).

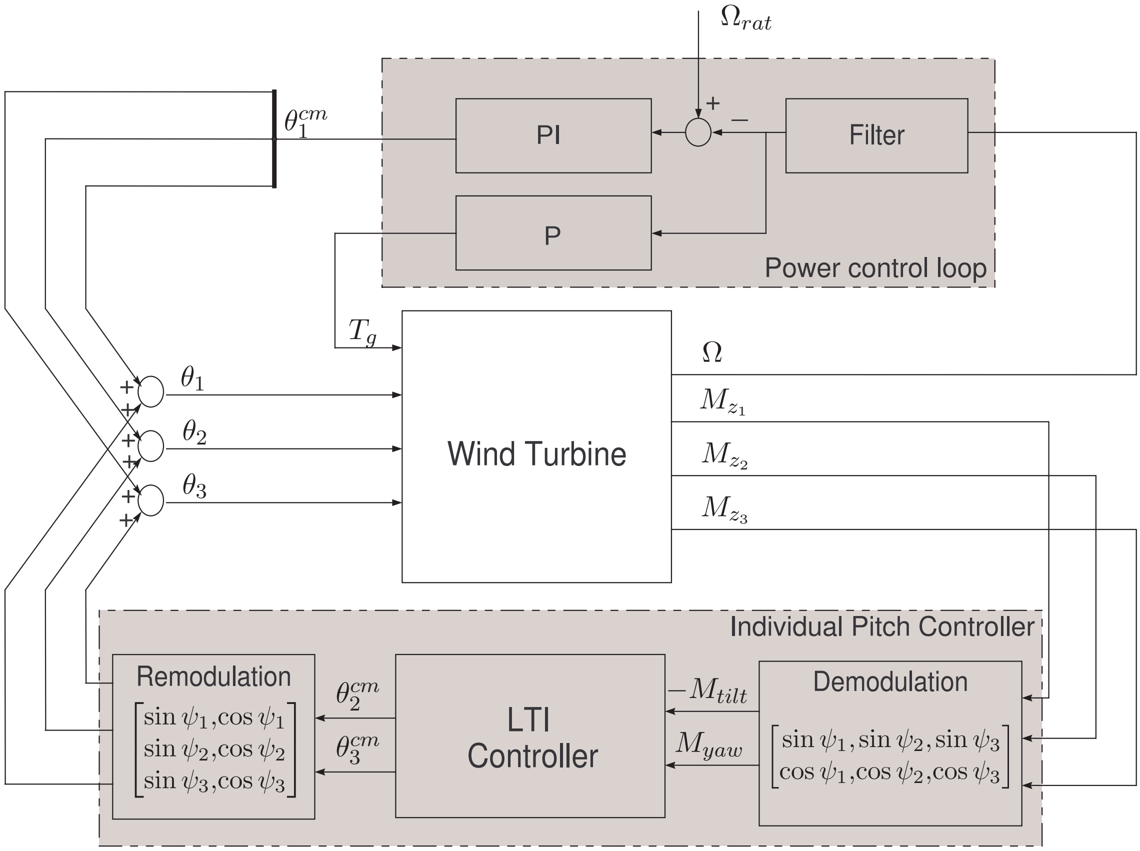

Figure 16: *Layout of the complete control structure*

For the latter the following creation scheme for 'artificial measurement signals' $\delta M_{z_{cm2}}$ and $\delta M_{z_{cm3}}$ has been utilized.

$$\begin{bmatrix} \delta M_{z_{cm2}} \\ \delta M_{z_{cm3}} \end{bmatrix} = \begin{pmatrix} \frac{2}{3}\sin\psi_1 & \frac{2}{3}\sin\psi_2 & \frac{2}{3}\sin\psi_3 \\ \frac{2}{3}\cos\psi_1 & \frac{2}{3}\cos\psi_2 & \frac{2}{3}\cos\psi_3 \end{pmatrix} \cdot \begin{bmatrix} \delta M_{z_1} \\ \delta M_{z_2} \\ \delta M_{z_3} \end{bmatrix} \tag{79}$$

while pitch angle additions are obtained via a modulation scheme of artificial control signals θ_2^{cm} and θ_3^{cm}.

$$\begin{bmatrix} \theta_1 \\ \theta_2 \\ \theta_3 \end{bmatrix} = \begin{pmatrix} \sin\psi_1 & \cos\psi_1 \\ \sin\psi_2 & \cos\psi_2 \\ \sin\psi_3 & \cos\psi_3 \end{pmatrix} \cdot \begin{bmatrix} \theta_2^{cm} \\ \theta_2^{cm} \end{bmatrix} \tag{80}$$

The frequency responce for the multivariable control technique is compared with classic PI control [van Engelen and Van der Hooft (2003)] for tilt and yaw moment control in the Coleman domain and is shown in Fig. 15. It can be clearly seen from the figure that conventional IPC approach (red dashed and dottedline) has good load reduction only at very low frequencies, while at 1P and higher there is completely no reduction, and even slight increase. The low frequency reduction is due to the integrator structure of this control method, making the method suitable for blade load reduction (as 0p reduction in M_{tilt} and M_{yaw} corresponds to 1P reduction in the flap-wise blade root bending moments), but cannot achieve fatigue-relevant load reduction on the non-rotating components of the wind turbine. On the other hand, by trading-off low-frequency load reduction, the proposed feedback-feedforward method achieves reduction over a much wider frequency range, including the

3p frequency which is very relevant for fatigue on the non-rotating components, such as the nacelle, yaw bearing and tower. And improved reduction at low frequencies can be obtained by including integral action in the controller.

4.4 Time domain simulation

Time domain simulations were performed with the controlled model. They were driven by blade effective wind input signals and three scenarios were addressed.

- Collective pitch only (Run 1).
- Collective pitch and IPC with integral action (Run 2)[van Engelen and Van der Hooft (2003)].
- Collective pitch and IPC with LQG (Run 3).

The model parameters pertain to a typical 2.5 MW wind turbine with 45m rotor radius R_b, 70 m tower height H, overall drive train inertia J_t of $12 \cdot 10^6 kgm^2$, and 1^{st} tower eigen frequency of 0.35 Hz. The parameters were determined for a wind speed of 18 m/s with a turbulence intensity of 0.1, rotor speed of 15 rpm and pitch angle of $10°$. Parasitical dynamics by pitch actuation, sensor and data processing were catered via an overall delay loop of 0.2 s.
The wind signal used in the simulation is as shown in Fig. 17

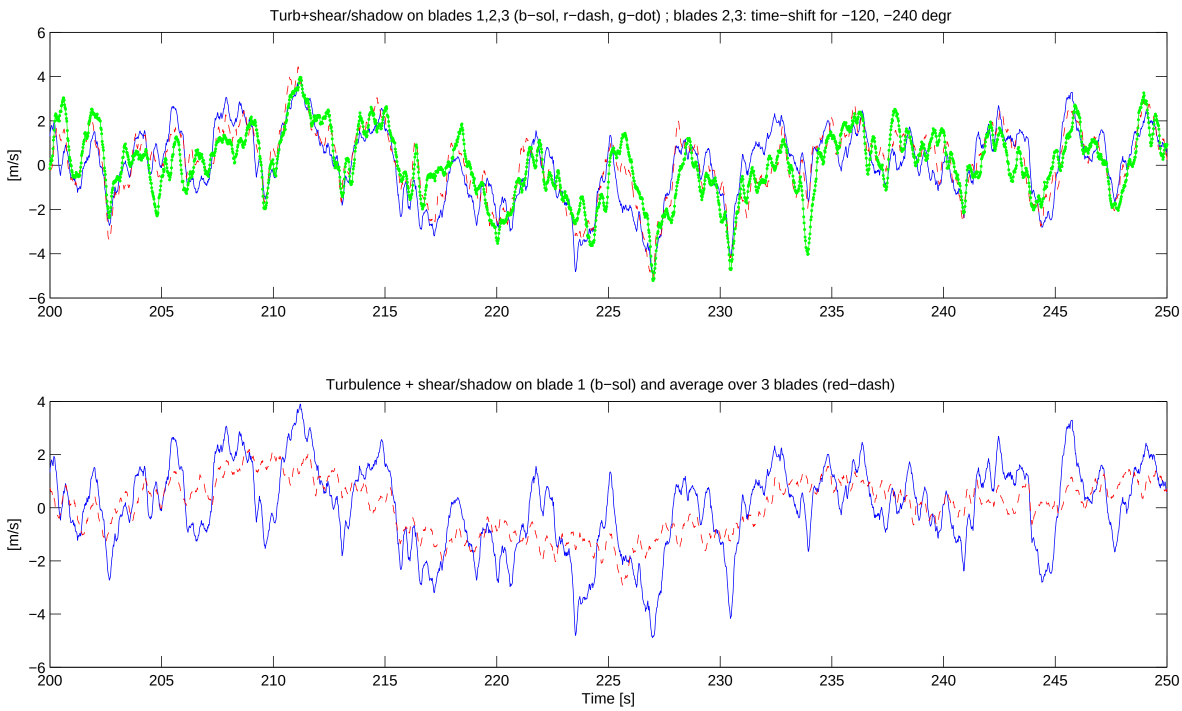

Figure 17: *Wind signal used in the simulations.Courtesy: [van Engelen (2006)]*

Each box in the following figures always contains the results for collective pitch only (Run 1) as blue (dark) line. The results with addition of individual pitch control to collective pitch control are plotted using red (light) line (Run 2 and Run 3). The graphs are generally plotted as a comparison of the two different IPC control techniques. Hence each plot is a comparison between one method of IPC (red line) to that of collective pitch control only (blue line). Run 1, Run 2 and Run 3 specify Collective pitch control only, IPC with integral action and IPC with LQG respectively.
Fig. 18 shows the time domain realisation of the tilt and yaw moments at the rotor center. The two boxes of time domain realisation for tilt and yaw moments pertain to different IPC control loop super imposed with collective pitch control only. The same holds for Fig. 19. From the figures it is clear that LQG algorithm reduces the loads for both 0p and 3p frequencies whereas the integral control increases the loads at modes with frequency higher than the eigen frequencies (0. 35 Hz) but has a very good load reduction capability at 0p. Fig. 20 shows the power spectra of the blade root flap

moment and pitch angle acceleration induced due to IPC. from the figure it is clear that again Integral control has a better load reduction capability at 1P frequency. But LQG control technique has its advantage that it has load reduction capability for a larger frequency range than the integral control loop and it is also less aggressive than Integral control when it comes to pitch actuation as shown by Fig. 20

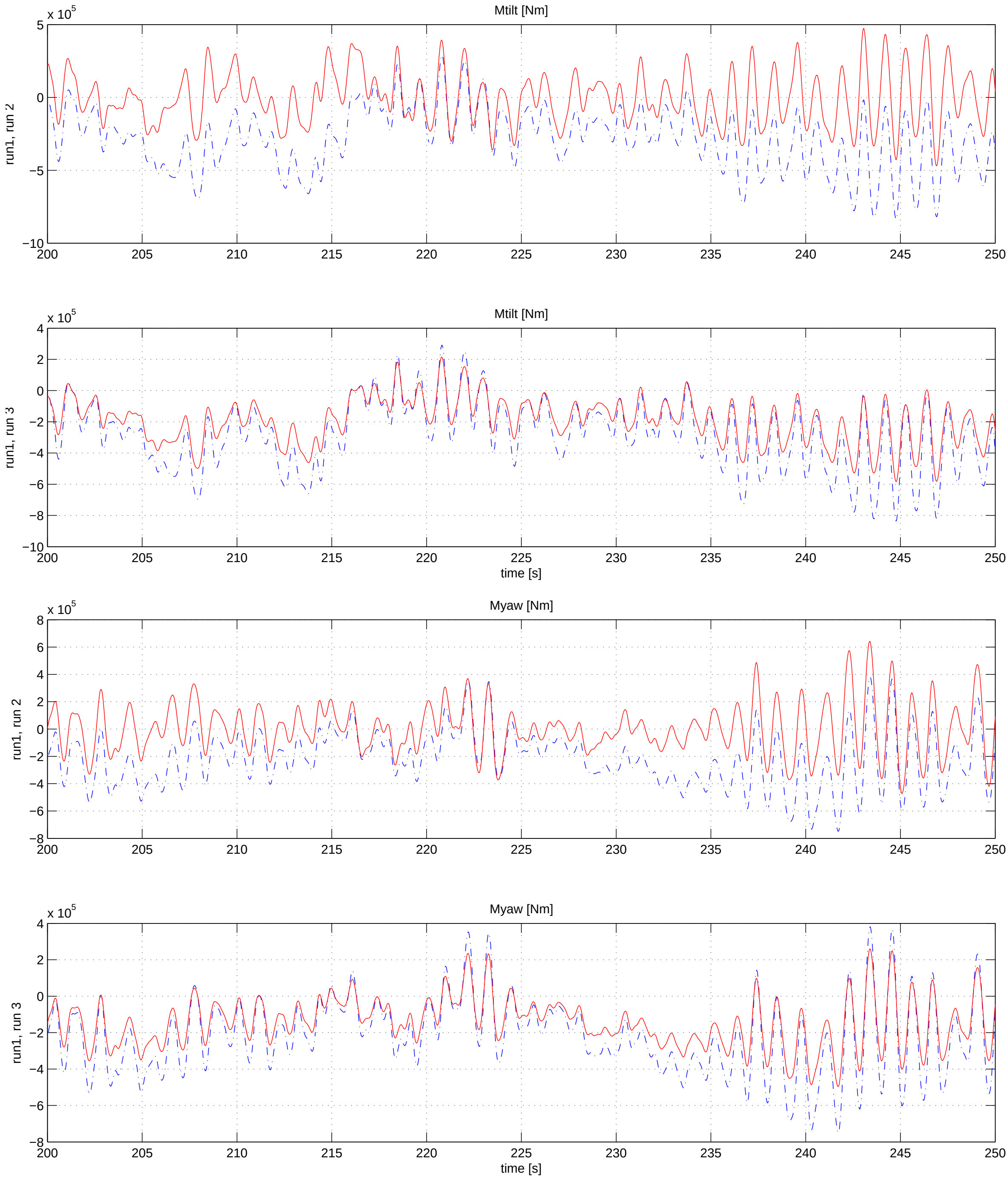

Figure 18: *Realisation of tilt (above) and yaw (below) moment in the rotor center with a wind speed of 18 m/s - The realisations are for the two different methods of IPC(solid) to CPC only (dashed), PI based IPC being Run 2 and LQG based IPC being Run 3 with CPC being Run 1.*

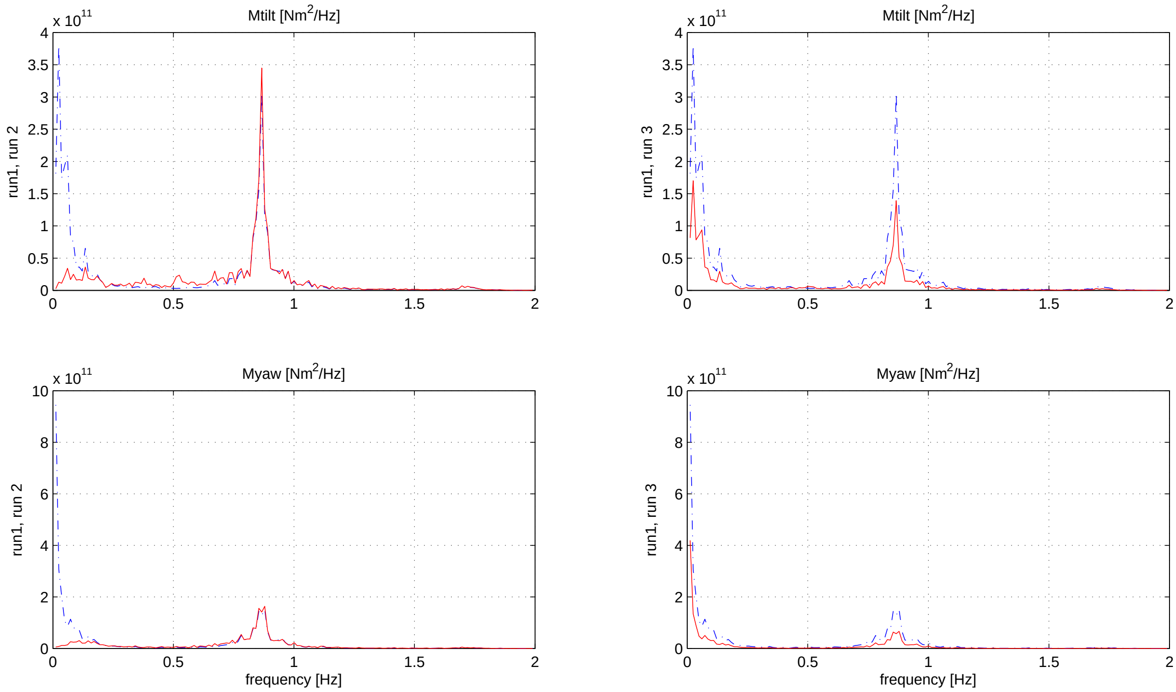

Figure 19: *Power spectra of tilt (above) and yaw (below) moment in the rotor center with a wind speed of 18 m/s*

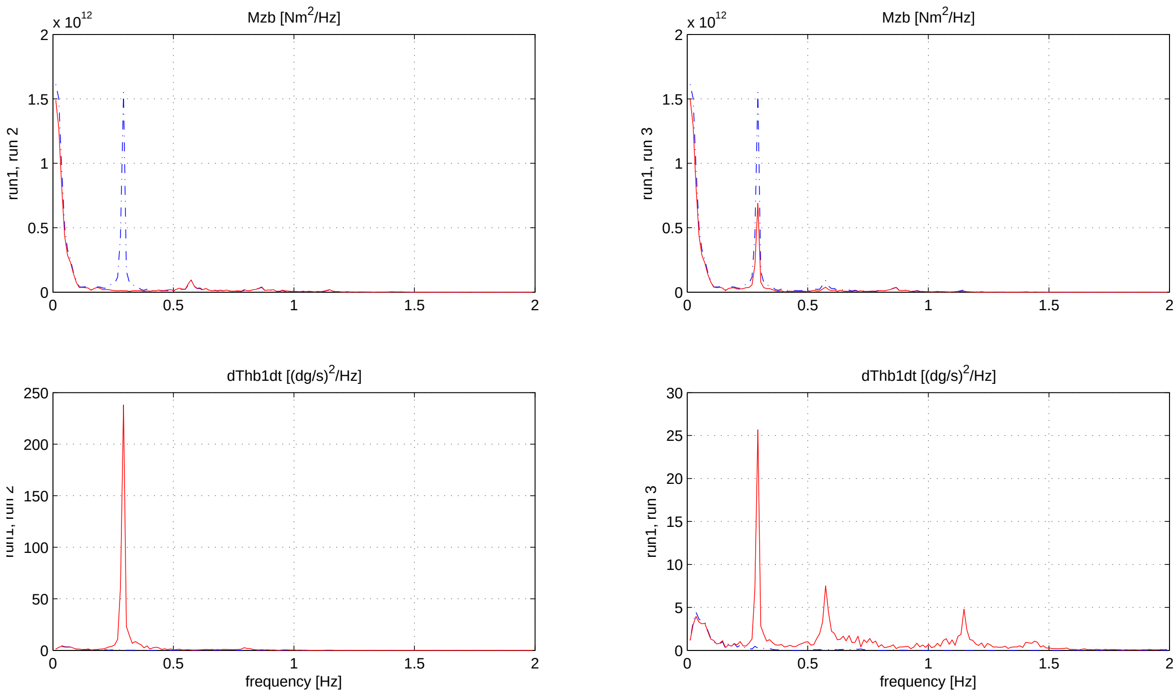

Figure 20: *Power spectra of flap moment (above) and pitch angle acceleration (below) with a wind speed of 18 m/s*

4.5 Controller analysis and results

The purpose of IPC control is to reduce loading of the blades and hence to reduce fatigue damage at above rated conditions. Hence it is necessary to analyse the standard deviation of the different loads experienced by the blades and tower. This is given in Tab. 1. From the table it is clear that both forms of IPC have good overall load reduction capabilities as they reduce the overall load by around 20%.

Table 1: *Standard deviation results of load simulations for the three controllers*

Controller	std(Mflap) [kNm]	std(Mtilt) [kNm]	std(Myaw) [kNm]
CPC only	341.9	211.6	217.3
IPC using PI technique	292.1	169.9	157.6
IPC using LQG technique	299.5	144.3	144.8

Fig. 21 shows the Power spectra comparison between the two controllers. The realisation with PI controller is plotted in blue (dark) and the realisation of LQG controller is plotted in red (light). It can be seen from the figure that LQG control reduces the moment at all frequencies and is much better for fatigue reduction than PI control. The maximum pitch speed for IPC for PI control rises to 7 $^\circ/s$ from only 2 $^\circ/s$ for collective pitch control. But for LQG control the maximum pitch speed appears to be only 4 $^\circ/s$.

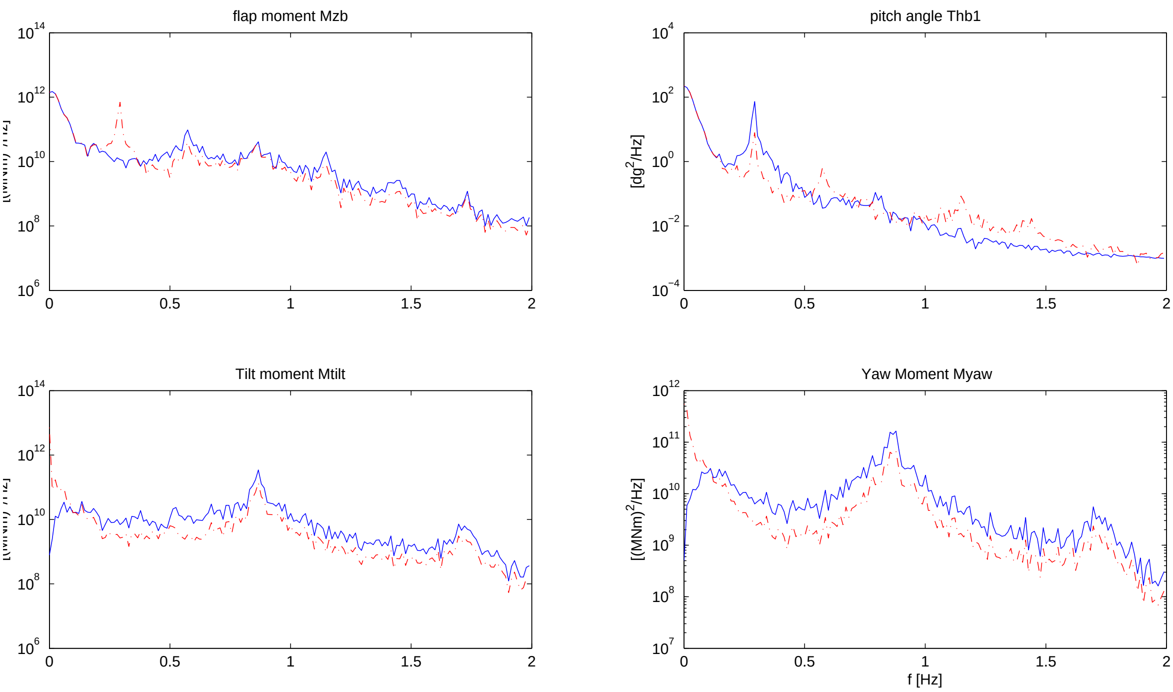

Figure 21: *Power spectra comparison of the two different control methods-PI (blue solid), LQG (red dashed)*

The main reason to use IPC for load reduction is to reduce fatigue damage caused by 1P effects caused by wind shear. A common industrial practice to compare fatigue load obtained under different conditions is to use an equivalent load range. Here a fatigue equivalent load cycle method, as explained by Hendriks and Bulder [Hendriks and Bulder (1995)], is used to compare the fatigue loads for the different control techniques. The reason being that this method takes into account mean level of the load cycles in addition to the equivalent load range , and hence provides a more thorough picture of fatigue the effect on fatigue load on a material. This method is meant to be used for the comparison and not for calculating the actual fatigue load damage. Hence the absolute value is less important than the ratio of the equivalent load range of two spectrums. The load spectrums of the flap moments M_{zb} are transformed into 1 Hz equivalent fatigue loads and mapped to fatigue damage via the method of Palmgren and Miner. The achieved reduction in fatigue damage is shown in Tab. 2 for different values of slope m (3 or 4 for steel; 10 or 11 for reinforced plastic).

Table 2: *1 Hz equivalent loading of flap moment M_{zb}(in kNm) for the three controllers*

Controller / slope no	3	4	10	11
CPC only	$5.702 \cdot 10^2$	$7.074 \cdot 10^2$	$1.280 \cdot 10^3$	$1.339 \cdot 10^3$
IPC using PI technique	$4.613 \cdot 10^2$	$5.870 \cdot 10^2$	$1.139 \cdot 10^3$	$1.196 \cdot 10^3$
IPC using LQG technique	$4.605 \cdot 10^2$	$5.867 \cdot 10^2$	$1.105 \cdot 10^3$	$1.158 \cdot 10^3$

Generally the blades are made of composite materials hence slopes 10 and 11 are of importance. From the two tables Tab. 1 and 2 it can be seen that even though the standard deviation of blade flap moments for LQG control technique is higher than that of the conventional control its fatigue load reduction of blade flap is better.

4.6 Conclusion

A simple linear wind turbine model is designed, based on a multi blade coordinate transformation for the design of both rotor speed regulation and 1P individual pitch control. Two individual pitch control methods , one using scalar control theory (PI) and the other using modern control technique (LQG), were compared and their results for load reduction and fatigue damage reduction were analysed. Preliminary time-domain simulations in full load conditions predict an achievable reduction in fatigue damage of up to 10 to 20 % using IPC. It also shows that LQG control is more appropriate than scalar control in achieving significant load reduction with minimal pitch actuation and hence is more suitable for large scale wind turbines.

5 Analysis and model reduction of detailed design of 2.5 MW wind turbine

5.1 Introduction

The ECN computer code TURBU [van Engelen (2007)] generates elaborate linearised models for 3-bladed horizontal axis wind turbines. These models include considerable features that are necessary for control design and aero-elastic stability analysis, like bending and torsion deformation, (unsteady) aerodynamic and hydrodynamic conversion and wake dynamics.Model inputs for the drive-train and rotor blades are transformed into multi-blade coordinates before they enter the LTI-model and the LTI-model outputs from the drive-train and rotor blades are transformed back to rotating coordinates. A linear model is computed for a certain aerodynamic equilibrium state. The latter is derived via the Blade Element Momentum theory. The average deformation state is matched to the aerodynamic equilibrium. This is based on non-linear propagation of the deformation of the individual elements caused by the average loading; the average deformation per element is based on slender beam bending theory. The basic design ideology of the wind turbine model derived from TURBU is shown in Fig. 22. The multibody wind turbine model so generated has 14 blade elements with 5 degrees of freedom for each blade element and 15 support elements with 5 degrees of freedom for the tower.

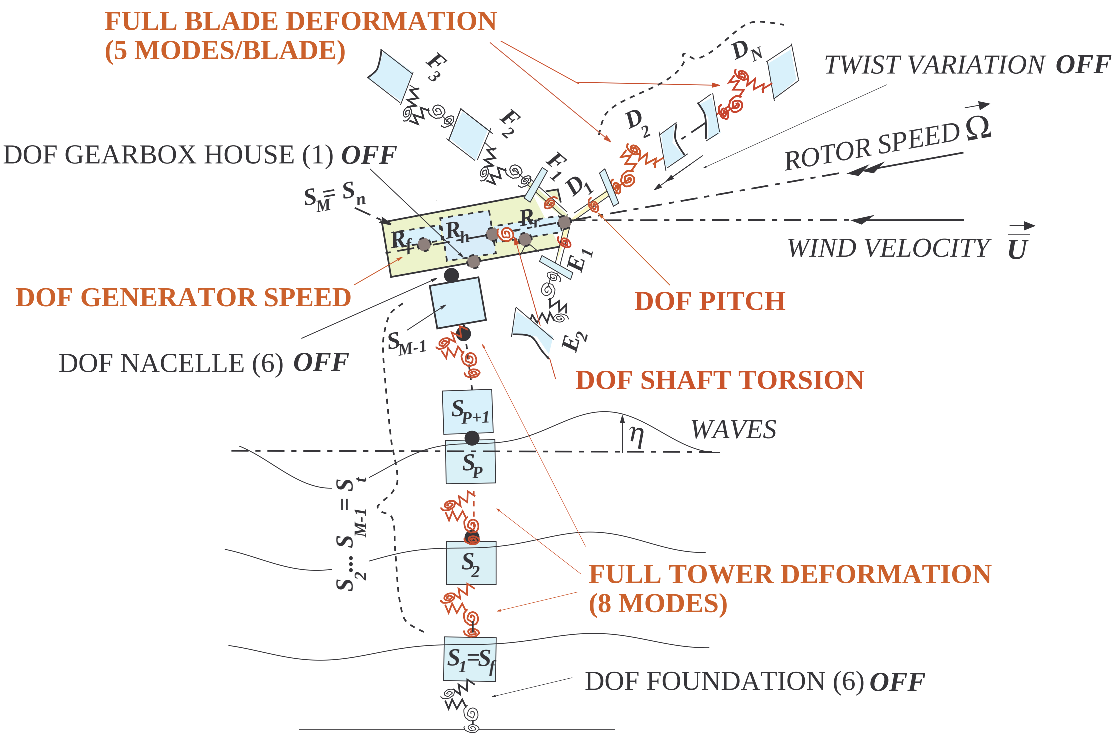

Figure 22: Wind turbine multibody model generated by TURBU. Courtesy: [van Engelen (2007)]

5.2 Model reduction for control design

The high-order sub models for the rotor blades and the tower are reduced. This is based on elimination of high-frequency modal modes in accordance with the approach adopted by Hurty and Craig & Bampton. This way we can reduce the model order significantly without any loss in accuracy in the dynamic behavior of the lower bending modes. Individual pitch control is used to reduce 1p bending modes which occur at around 0.35 Hz frequency. Hence it is enough that we take into account a low order model that maps only the low frequency behavior of the turbine. The TURBU program allows the user to choose distinct degrees of freedom in order to design a very low order model [van Engelen (2007)]. Hence for Individual pitch control the important degrees of freedom that are needed are 1 degree of freedom for each blade element (lumped blade model), one degree of freedom for the shaft (shaft torsion) and generator speed, and finally one degree of freedom for the tower. The reduced order lumped model as shown in Fig. 23.

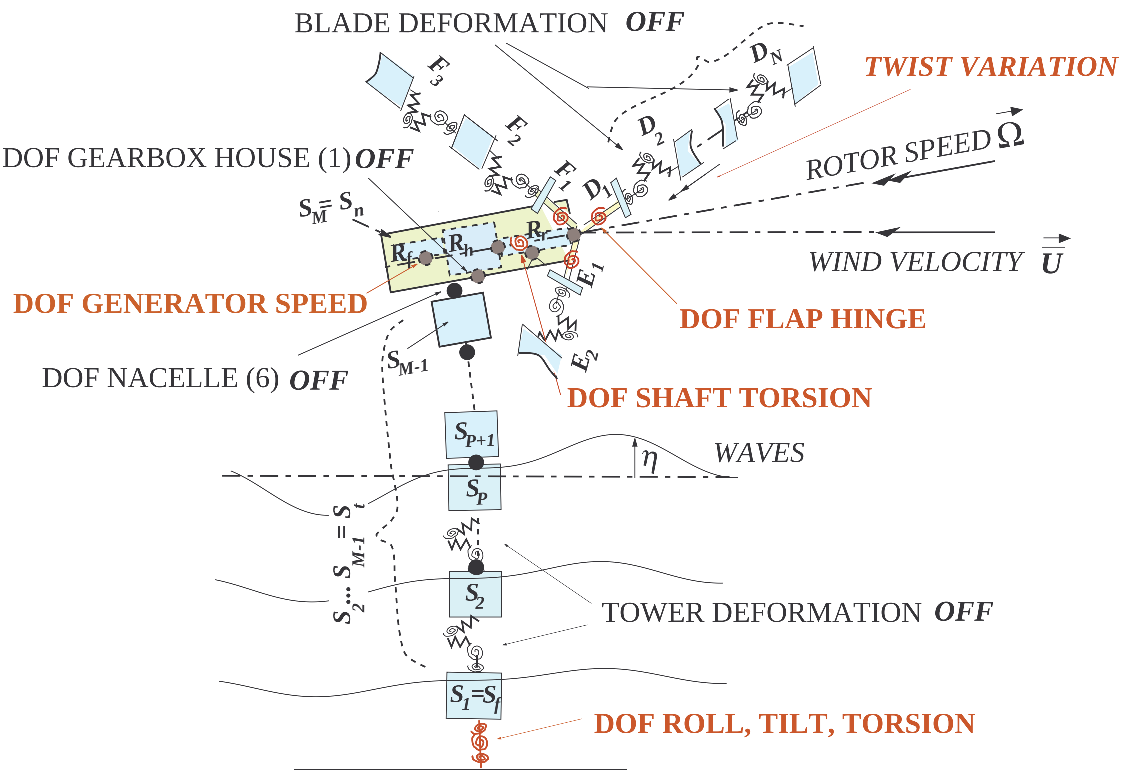

Figure 23: Wind turbine reduced order lumped model generated by TURBU (The DOF's in red are the included states and DOF's in black are omitted(denoted by term 'OFF')). Courtesy: [van Engelen (2007)]

The frequency response plots of the multibody and lumped model show that the lumped model has all the required dynamics at low frequencies (around 1p). It appears to be an appropriate choice for control design model which follows from the closed loop transfer function analysis as shown in Fig. 24.

5.3 Control design

For multivariable control the wind turbine system is derived from the reduced order lumped model and an augmented system is derived by adding a random walk model as explained in section 4.2.2. The Kalman filter provides an unbiased estimate of the whole augmented wind turbine system.
The controller gain is found out in a two fold manner as described in section 4.2.3. But here the pseudo feed forward gain is not static in nature as in the simplified wind turbine model. Since TURBU is a more detailed model and the fact that there is a coupling between the tilt and yaw moments, shows that the tilt and yaw moments have a large effect on the states of the wind turbine. Hence the feed

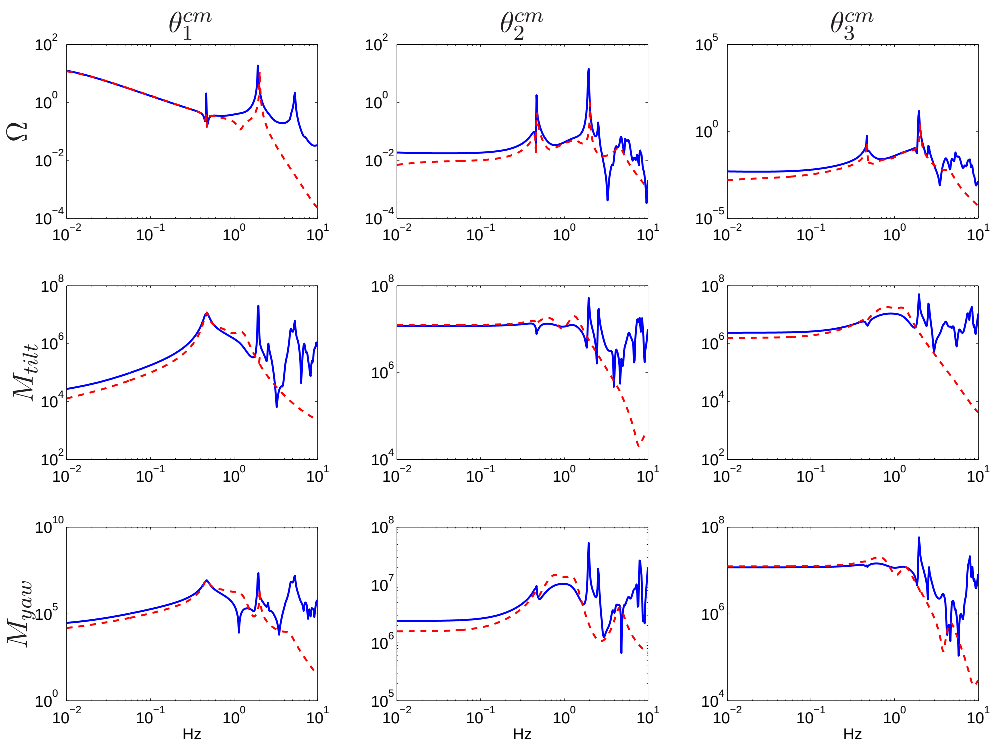

Figure 24: Frequency response from multi-blade pitch angles to rotor speed, tile moment and yaw moment, both for the multibody (blue-solid) and the lumped models (red-dashed)

forward compensation is actually a dynamic compensation technique. For dynamic compensation we need to invert the transfer function between θ_i^{cm} and $\delta M_{z_i^{cm}}$ (G(z)) as explained in Sec. 3.3.1.

5.4 Results and Conclusion

Conclusions similar to the one made in Section 4.3 can be made based on the results with the TURBU model, as depicted on Figure 25. Now there is coupling between tilt and yaw-oriented moment, so the off-diagonal channels are also plotted. Notice that, although the IPC controller design has been performed based on the reduced lumped TURBU model, the results on the figure represent the closed-loop system with the detailed multibody TURBU model. For comparison between the multivariable control technique and simple scalar control [van Engelen and Van der Hooft (2003)] the following implementation is followed.

- The same simple three scalar control loop, but with static decoupling inclusion [van Engelen (2007)] is implemented
- The new multivariable control technique explained in Sec. 5.3 is implemented

The feedback loop configurations are presented in appendix B. From the frequency response it can be seen that out of the two configurations, multivariable control has the maximal load reduction at around 1p frequency. This conclusion with the TURBU model agrees with the result already provided with the simplified wind turbine model.

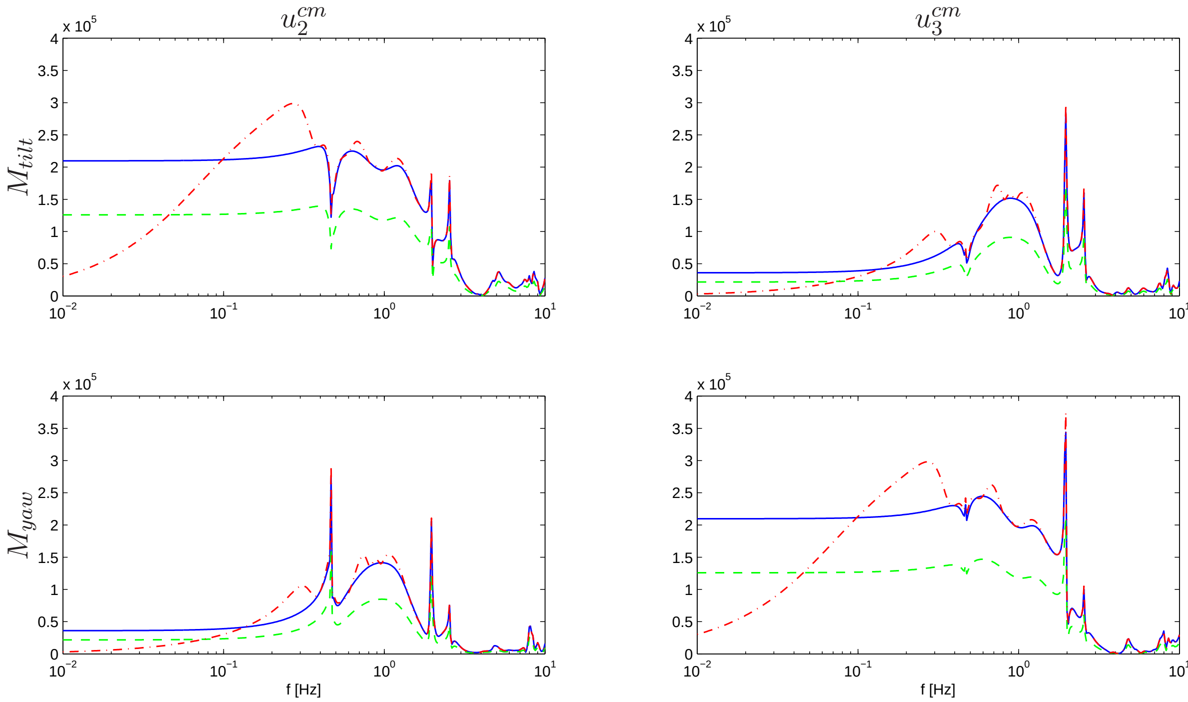

Figure 25: Frequency response plot of tilt moment M_{tilt} (first row) and yaw moment M_{yaw} (second row) due to the multi-blade wind inputs u_2^{cm} (left column) and u_3^{cm} (right column) for the TURBU model with no IPC (blue solid), conventional IPC (red dash-dotted) and new feedback-feedforward IPC (green dashed).

6 Conclusions and Recommendations

6.1 Conclusions

The present trend in the field of wind energy is to reduce the cost of energy production as much as possible with the help of wind turbines. This is done by increasing the size of the rotor blades and placing the wind farms in areas with the highest average wind speeds, for example offshore locations. With the increasing rotor diameter and moving them to locations where maintenance is difficult and expensive, active reduction of fatigue loads has become an important topic of research.

A very important factor that affects the fatigue loading is the 1P loading of the rotor blades due to wind shear, tower shadow and skew inflow. Hence the objective of this thesis was to develop a controller that could reduce the blade loading for this kind of disturbances. Multivariable control utilising a LQG control technique and feed forward disturbance rejection technique were applied for this purpose.

The main issue addressed in this thesis was to show that multivariable control technique can be successfully implemented to reduce 1P loads and in turn be used to reduce fatigue loads. This was achieved by addressing the following issues

- Development of a wind speed model
- Design of a basic Controller structure
- Design of a feed forward Controller for wind disturbance rejection

Development of a wind speed model Wind speed variations are difficult to measure and pitot tubes used for wind speed measurements have robustness issues. Hence we need to have a model to simulate the wind signals. In this thesis a simple random walk model has been suggested and implemented. The advantage of this model is that this model is linear and can simulate the low frequency behavior of the wind turbine fairly accurately and reduces costs involved with system identification for determining models for wind signals.

Design of a basic Controller structure The control design for IPC was solved in a two stage manner by a) determining optimal feedback gains for the wind turbine states and b) coupling it with (pseudo) feed forward gain for wind disturbance rejection. This coupled gain is then added to the Kalman filter derived for the whole wind turbine system (including the random walk model for the wind signal) to form a LQG controller.

Design of a feed forward Controller for wind disturbance rejection The feed forward gain for wind disturbance was found to be static for the simple turbine model but, for the more complex TURBU model, a dynamic feed forward controller was needed.

Finally the multivariable controller was compared with three scalar loop controller [van Engelen and Van der Hooft (2003)] and the following results were obtained

- The three scalar loop controller has a much better 1P blade loading reduction (static load reduction) when compared to multivariable controller
- At 2P blade loading and 3P nacelle loading frequencies, the multivariable controller has much better load reduction capabilities and hence much higher fatigue reduction.
- Analysis with the TURBU model it was seen that the scalar controller could not reduce the loads around the 1P- frequency in fixed frame coordinates (2P frequency in the blade coordinates) because of the coupling of the tilt and yaw moments at 1P frequency which was taken into account by the multivariable controller

Hence even though scalar approach has much better zero frequency load reduction the multivariable controller is much better when it comes to load reduction at blade loading and nacelle loading frequencies and is hence better suitable for fatigue load reduction.

6.2 Recommendations

6.2.1 Overall Control Structure

In this thesis the IPC control loop was added in parallel to collective pitch control and generator torque control loops. Presently, wind turbine control is separated in two distinct operation areas. At below-rated operation the torque controller is active and the pitch demand is fixed at optimal pitch, while in above-rated operations the pitch controller is active and the torque demand is fixed at rated. Around rated conditions, additional logic is applied so that production losses are kept minimal during the switch. Further, IPC is added to the control setup in above rated conditions for load reduction. This means a total of three controllers is used independent of each other in order to maximise power generation and reduce blade loads at the same time. But, by using multivariable control techniques we can lump these three different controllers into a single controller and thereby improve the power production. This coupling of CPC and IPC, in a multivariable control concept setup will also eliminate the coupling effect that is present between the two control loops.

6.2.2 Improvement of 1P blade loading frequency load reduction using weighting frequencies

The present control technique reduces the blade moments over the whole frequency range. But the actuators do not function at those frequencies and hence the control effort utilised to reduce high frequency loads is actually wasted. Hence weighting filters can be added to the controller so that only low frequency loads are reduced and there by zero frequency load reduction is enhanced.

6.2.3 LPV modeling and control

The presented control approach follows a linearised wind turbine model. But the wind turbine as such is a non-linear system. Hence a LPV controller taking into account the non linearities can be designed and this would greatly reduce the complexity of the control structure for the different operation zones and simplify the control structure for overall control of the wind turbine.

It is also recommended to

- Include blade bending and unsteady aerodynamics in the control synthesis approach;
- Simulate the control configuration with a nonlinear wind turbine model like PHATAS.

Literatuurlijst

Archer, C. and M. Jacobson (2005): *Evaluation of global wind power*. Journal of Geophysical Research, Vol-110:212–216.

Bossanyi, E. (2000): *The design of closed loop controllers for wind turbine*. Wind Energy, 3:149–163.

Bossanyi, E. (2003a): *Individual blade pitch control for load reduction*. Wind Energy, 6:119–128.

Bossanyi, E. (2003b): *Wind turbine control for load reduction*. Wind Energy, 6:229–244.

Bossanyi, E. (2005): *Further load reduction with Individual pitch control*. Wind Energy, 8:481–485.

Caselitz, P., W. Kleinkauf, W. Krueger, J. Petschenka, M. Reichardt and K. Stoerzel (1997): *Reduction of fatigue loads on wind energy converters by advanced controlmethods.* Proc. European Wind Energy Conference, Dublin. pages 555–558.

Coleman, R. and A. Feingold (1958): *Theory of Self-excited Mechanical Oscillations of Helicopter Rotors withHinged Blades*. USGPO.

Doyle, J. (1983): *Synthesis of robust controllers and filters*. IEEE conference on Decision and Control. pages 109–114.

George, K., M.Verhaegen and J. Scherpen (1999): *A systematic and Numerically Efficient Procedure For Stable Dynamic Model Inversion of LTI Systems*. 38th Conference on Decision and Control. Pheonix, Arizona USA, pages 1881–1886.

Hansen, M. (2000): *Aerodynamics of Wind Turbines*. James & James.

Hansen, M. (2003): *Aeroelastic Stability Analysis of Wind Turbines using an Eigen value approach*. European Wind Energy Conference. Madrid, Spain.

Hendriks, H. and B. Bulder (1995): *Fatigue Equivalent Load Cycle Method - A general method to compare the fatigue loading of different load spectrums*. Report ECN-C–95-074, ECN.

Johnson, W. (1982): *Self-Tuning regulators for Multicyclic Control of Helicopter vibration*. Report, NASA.

van Kuik, G., T. van Holten, M. Verhaegen and S. Dijkstra (2003): *Smart dynamic rotor control of large offshore wind turbines*. Report, Technologiestichting STW.

Larsen, T., H. Madson and K. Thomson (2005): *Active load reduction using individual pitch, based on local blade flowmeasurements*. Wind Energy 2005, 8:67–80.

Lovera, M., P. Colaneri, C. Malpica and R. Celi (2003): *Closed-loop stability analysis of HHC and IBC, with application to a hingelessrotor helicopter*. 29th European Rotorcraft Forum.

Lovera, M., P. Colaneri, C. Malpica and R. Celi (2004): *Discrete-time, closed loop aeromechanical stability analysis of helicopterswith higher harmonic control*. 60th Annual forum of the American Helicopter Society.

Mesic, S., V. Verdult, M. Verhaegen and S. Kanev (2003): *Estimation and Robustness analysis of actuator faults based on kalman filtering*. 5th Symposium on Fault Detection, Supervision. Washington, D.C., USA.

Skogestad, S. and I. Postelwithe (2005): *Multivariable feedback control; analysis and design*. John Wiley and Sons.

Stol, K. (2003): *Disturbance tracking and blade load control of wind turbines in variablespeed operations*. Report, NREL.

Van der Hooft, E., P. Schaak and T. van Engelen (2003): *Wind turbine control algorithm*. Report ECN-C–03-111, ECN.

van Engelen, T. (2006): *Design Model and Load Reduction Assessment for Multi-rotational Mode Individual Pitch Control (Higher Harmonics Control)*. European Wind Energy Conference. Athens, Greece.

van Engelen, T. (2007): *Control design based on aero-hydro-servo-elastic linear models from TURBU*. European Wind Energy Conference 2007. Milano,Italy.

van Engelen, T. and E. Van der Hooft (2003): *Individual pitch control inventory*. Report ECN-C–03-138, ECN.

Verhaegen, M. and V. Verdult (2005): *Filtering and System Identification: An Introduction*. SC4040. TU Delft, Delft, Netherlands.

Watson, R. (2001): *IPCC Third Assessment Report: Climate Change 2001*. Report, IPCC,Geneva.

Wright, A. (2004): *Modern Control Design for Flexible Wind Turbines*. Report, NREL.

Wright, A. and M. Balas (2002): *Design of state space based control algorithms for wind turbine speed regulations*. Report, NREL.

Wright, A. and M. Balas (2003): *Design of controls to attenuate loads in the controls advanced researchturbine*. Report, NREL.

A Proof

A.1 Stationarity of multi-blade wind speeds

Theorem Under the assumption homogeneous turbulence, constant rotational speed and non-oblique oriented wind flow, the multi-blade components u_i^{cm}, $i = 1, 2, 3$, of the blade effective wind speeds are stationary processes.

proof For homogeneous turbulence and purely axial wind direction, the blade effective wind speed u_i, experienced on a fixed point on a rotating blade, can be expressed in the form of a time-varying Fourier expansion

$$u_i(t, \psi_i) = \sum_{p=-\infty}^{\infty} e^{jp\psi_i(t)} \hat{u}_p(t), \tag{81}$$

where $\psi_i(t)$ is the azimuth angle of blade i, and

$$\hat{u}_p(t) = \frac{1}{2\pi} \int_0^{2\pi} e^{jp\phi} u(t, \phi) d\phi \tag{82}$$

are time-dependent rotational modes. It has been shown in [van Engelen (2006)] that the following expression holds for the multi-blade coordinates of the blade effective wind speeds

$$\begin{bmatrix} u_1^{cm}(t) \\ u_2^{cm}(t) \\ u_3^{cm}(t) \end{bmatrix} = \sum_{m=-\infty}^{\infty} e^{j3m\psi} \begin{bmatrix} \hat{u}_{3m}(t) \\ j(\hat{u}_{3m+1}(t) - \hat{u}_{3m-1}(t)) \\ j(\hat{u}_{3m+1}(t) + \hat{u}_{3m-1}(t)). \end{bmatrix} \tag{83}$$

Then, with a^* denoting the conjugate of a, it can easily be shown that

$$\begin{bmatrix} u_1^{cm}(t+\tau) \\ u_2^{cm}(t+\tau) \\ u_3^{cm}(t+\tau) \end{bmatrix}^* = \sum_{n=-\infty}^{\infty} e^{-j3n\psi} \begin{bmatrix} \hat{u}_{3n}(t+\tau) \\ -j(\hat{u}^*_{3n+1}(t+\tau) - \hat{u}^*_{3n-1}(t+\tau)) \\ -j(\hat{u}^*_{3n+1}(t+\tau) + \hat{u}^*_{3n-1}(t+\tau)) \end{bmatrix}. \tag{84}$$

Therefore, for the variance of u_2^{cm} one has

$$\begin{aligned} & E\{u_2^{cm}(t)(u_2^{cm}(t+\tau))^*\} \\ & = E\left\{ \sum_{m,n=-\infty}^{\infty} e^{j3(m-n)\psi} \left(\hat{u}_{3m+1}(t) - \hat{u}_{3m-1}(t)\right) \left(\hat{u}^*_{3n+1}(t+\tau) - \hat{u}^*_{3n-1}(t+\tau)\right) \right\} \\ & = \sum_{m,n=-\infty}^{\infty} e^{j3(m-n)\psi} E\left\{ \left(\hat{u}_{3m+1}(t) - \hat{u}_{3m-1}(t)\right) \left(\hat{u}^*_{3n+1}(t+\tau) - \hat{u}^*_{3n-1}(t+\tau)\right) \right\} \end{aligned} \tag{85}$$

since under assumption of constant rotational speed one has that $\psi = \Omega t + \psi(0)$, so that $e^{j3(m-n)\psi}$ are purely deterministic signals. Furthermore, in [van Engelen (2007)] it is proved that, under the considered assumptions, the rotational modes are orthogonal and stationary, i.e.

$$E\left\{\hat{u}_p(t)\hat{u}_q^*(t+\tau)\right\} = \delta(p-q)\sigma_{\hat{u}_p}(\tau), \tag{86}$$

where $\delta(\cdot)$ denotes the Dirac's delta function, and $\sigma_{\hat{u}_p}(\tau)$ is the correlation function of $\hat{u}_p$. Therefore, in the above expression for $E\{u_2^{cm}(t)(u_2^{cm}(t+\tau))^*\}$ all terms for $n \neq m$ drop, giving

$$E\{u_2^{cm}(t)(u_2^{cm}(t+\tau))^*\} = \sum_{m=-\infty}^{\infty} (\sigma_{\hat{u}_{3m-1}}(\tau) + \sigma_{\hat{u}_{3m+1}}(\tau)). \tag{87}$$

Clearly, the correlation function of $u_2^{cm}(t)$ is not a function of the time t. The same lines can be followed for the first and third multi-blade components $u_1^{cm}(t)$, and $u_3^{cm}(t)$ to arrive at the same conclusion. Therefore, $u_i^{cm}(t)$, $i = 1, 2, 3$, are stationary processes under the mentioned assumptions.

A.2 Observability of random walk model

Theorem The augmented system given by Eq. 70 is observable **iff (A,C)** is observable, and $C(\lambda I - A)^{-1}F\Gamma\xi \neq 0 \; \forall$ eigenvalues $\lambda \in \mathbb{C}$ and eigenvectors $\xi \in \mathbb{C}^p$ of Φ, provided the eigenvalues of Φ are different to that of **A**.

proof This proof is basically derived from [Mesic et al. (2003)]. According to Popov-Belevitch-Hautus (PBH) test for checking observability, the augmented system Eq. 70 is observable if for all eigen values of the system denoted as below

$$\begin{bmatrix} A & F\Gamma \\ 0 & \Phi \end{bmatrix} \begin{bmatrix} \eta \\ \xi \end{bmatrix} = \lambda \cdot \begin{bmatrix} \eta \\ \xi \end{bmatrix} \tag{88}$$

the condition:

$$\begin{bmatrix} C & 0 \end{bmatrix} \begin{bmatrix} \eta \\ \xi \end{bmatrix} = 0 \tag{89}$$

iff $\left[\eta^T \xi^T\right]^T = 0$.

From the lower part of it follows that: $\xi = 0$ or λ is an eigenvalue of Φ. With $\xi = 0$ it follows from Eq. 88 that A$\eta = \lambda\eta$ and according to the PBH test Cη can only be zero provided that η is zero, since the pair (A,C) is observable. With λ an eigenvalue of Φ the top row of 88 reads: $(\lambda I - A)\eta = F\Gamma\xi$ and therefore $\eta = (\lambda I - A)^{-1}F\Gamma\xi$ since λ is not an eigenvalue of A. Hence C$\eta = 0$ implies $C(\lambda I - A)^{-1}F\Gamma\xi = 0$ but this can only hold provided that $\eta = 0$, and hence proved.

B Feedback loops

The graphical representation of feedback loops for the two different individual pitch control is provided here.

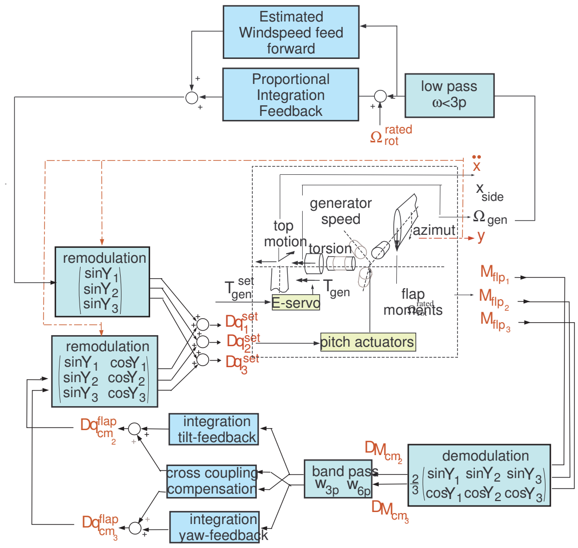

Figure 26: Layout of Control loop for three scalar control with static decoupling. Courtesy: ir. T.G. van Engelen

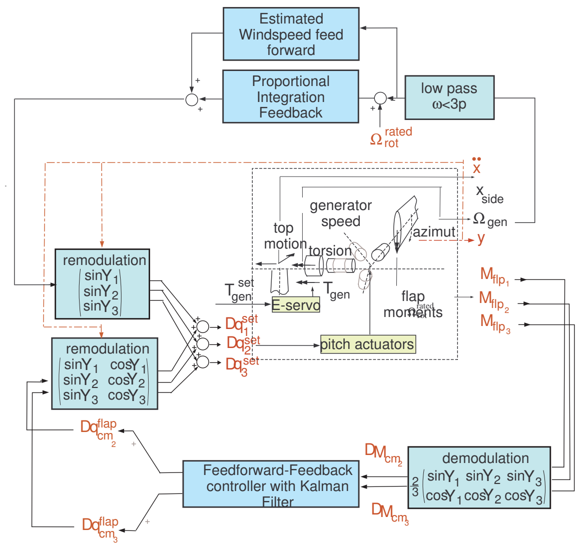

Figure 27: Layout of kalman estimator based multivariable control loop. Courtesy: ir. T.G. van Engelen